Superstructure Optimization of Multiple Cyclone Arrangements Using Mixed Integer Nonlinear Programming

by

Muhamad Fariz Failaka

A thesis
presented to the University of Waterloo
in fulfillment of the
thesis requirement for the degree of
Master of Applied Science
in
Chemical Engineering

Waterloo, Ontario, Canada, 2015

© Muhamad Fariz Failaka 2015

I hereby declare that I am the sole author of this thesis. This is a true copy of the thesis, including any required final revisions, as accepted by my examiners.

I understand that my thesis may be made electronically available to the public.

Abstract

The gas-solid cyclone has been remarkably widely used among all types of industrial gas-cleaning devices. Many studies have been conducted and reported excessive experimental, theoretical, and computational research aimed at understanding and predicting the performance of cyclones. However, the majority of these works have only focused on the development of single cyclones. In the meantime, the use of multiple cyclones can be considered as one solution to the demands of obtaining the best pollution control strategies to achieve a minimum level of pollution reduction. This has motivated the development of effective formulation for the cyclone arrangement problem. In this work a new optimization model of multiple cyclone arrangement is presented. The key idea is to present the capability of General Algebraic Modeling System (GAMS) software in obtaining the optimal number and dimensions of the cyclone, and the best cyclone arrangement for a certain condition with respect to the minimum total cost, including the operating cost and the capital cost.

The proposed model of nonlinear programming (NLP) and mixed integer nonlinear programming (MINLP) has been successfully applied to different case studies. The NLP model is applied to an NPK (Nitrogen, Phosphorus, and Potassium) fertilizer plant to find the optimal number and dimensions of the 1D3D, 2D2D, and 1D2D cyclones arranged either in parallel or series. In another case study with the total flow rate of 165 m^3/s of a stream to be processed in a paper mill, the best cyclone arrangement of parallel-series for three different combinations of the 1D3D and 2D2D cyclone is obtained through the use of MINLP modeling. The results show that different types of cyclones, applied in NPK fertilizer plant, result in different optimal numbers of cyclones. Each type of cyclone (i.e., 1D3D, 2D2D, and 1D2D) has an alternative that can be arranged either in parallel or in series configuration. Furthermore, different values used for the upper bound of D and N in the proposed MINLP model, result in a different cyclone arrangement of parallel-series selected as the optimal solution. The cyclone of 2D2D+2D2D arranged in parallel-series is found to be more economical and efficient compared to other arrangements.

iv

Dedicated to my parents, and my beloved family

Table of Contents

List of Tables

x

List of Figures

Nomenclature

Δt the required time for the particle to reach the bottom of the cyclone (s)

ΔP the cyclone pressure drop

ΔP^L the lower bound of cyclone pressure drop

ΔP^U the upper bound of cyclone pressure drop

ΔP_k the pressure drop of each cyclone on level k

ΔP_k^U the upper bound of cyclone pressure drop on level k

ΔP_p the pressure drop of cyclone in parallel arrangement

ΔP_s the pressure drop of cyclone in series arrangement

ΔP_{k_1} the pressure drop of the first cyclone on level k

ΔP_{k_2} the pressure drop of the second cyclone on level k

ΔP_{max} the maximum pressure drop

η^L the lower bound of cyclone efficiency

η^U the upper bound of cyclone efficiency

η_1 the efficiency of the first cyclone in series arrangement

η_2 the efficiency of the second cyclone in series arrangement

η_3 the efficiency of the third cyclone in series arrangement

η_{1_k} the efficiency of the first cyclone on level k

η_{2_k} the efficiency of the second cyclone on level k

η_{ov} the overall efficiency of series arrangement

η_{ov}^{L} the lower bound of overall efficiency of the arrangement

η_{ov}^{U} the upper bound of overall efficiency of the arrangement

η_{ov_k} the overall efficiency of the parallel-series cyclone arrangement on level k

η_{ov_t} the overall efficiency of the cyclone system

μ the viscosity of gas

ρ the gas density

ρ_p the particle density

a the inlet height (m)

a_0 the ratio of inlet height

a_i the decision variables

a_i^{L} the lower bound of decision variables

a_i^{U} the upper bound of decision variables

A_R the total inside area of the cyclone contributing to frictional drag

a_{1D3D_0} the ratio of inlet height of cyclone 1D3D

a_{2D2D_0} the ratio of inlet height of cyclone 2D2D

B the dust outlet diameter (m)

b the inlet width (m)

B_0 the ratio of dust outlet diameter

b_0 the ratio of inlet width

$b_{(1D3D)}$ the inlet width of cyclone 1D3D

$b_{(2D2D)}$ the inlet width of cyclone 2D2D

b_{1D3D_0} the ratio of inlet width of cyclone 1D3D

b_{2D2D_0} the ratio of inlet width of cyclone 2D2D

C_B the known base cost for cyclone with diameter D_B

c_e the cost of utilities (\$/J)

c_{cap} the capital cost (\$/s)

c_{opr} the operating cost (\$/s)

c_{tot} the total cost (\$/s)

c_{tot_p} the total cost of parallel cyclone arrangement

c_{tot_s} the total cost of series cyclone arrangement

D the diameter of the cyclone (m)

D^L the lower bound of cyclone diameter

D^U the upper bound of cyclone diameter

D_B the cyclone base diameter

D_e the gas outlet or vortex finder diameter (m)

D_k^U the upper bound of cyclone diameter on level k

D_p the diameter of cyclone in parallel arrangement

d_p the cut size diameter

D_p^U the upper bound of cyclone diameter in parallel lines

D_{CS} the core / control surface diameter

D_{e_0} the ratio of gas outlet or vortex finder diameter

D_{k_1} the diameter of the first cyclone on level k

D_{k_2} the diameter of the second cyclone on level k

d_{p_1} the cut-size diameter of the first cyclone in series arrangement

d_{p_2} the cut-size diameter of the second cyclone in series arrangement

d_{p_3} the cut-size diameter of the third cyclone in series arrangement

$d_{P_{(1D3D)}}$ the cut-size diameter of cyclone 1D3D

$d_{P_{(2D2D)}}$ the cut-size diameter of cyclone 2D2D

D_{s_1} the diameter of the first cyclone in series arrangement

D_{s_2} the diameter of the second cyclone in series arrangement

D_{s_3} the diameter of the third cyclone in series arrangement

$D_{(1D3D)_1}$ the diameter of the first cyclone 1D3D

$D_{(1D3D)_2}$ the diameter of the second cyclone 1D3D

$D_{(2D2D)_1}$ the diameter of the first cyclone 2D2D

$D_{(2D2D)_2}$ the diameter of the second cyclone 2D2D

$d_{p_{(1D3D)_1}}$ the cut-size diameter of the first cyclone 1D3D

$d_{p_{(1D3D)_2}}$ the cut-size diameter of the second cyclone 1D3D

$d_{p_{(2D2D)_1}}$ the cut-size diameter of the first cyclone 2D2D

$d_{p_{(2D2D)_2}}$ the cut-size diameter of the second cyclone 2D2D

e constant

F the investment factor

f the friction factor

F_d the drag force of the fluid on a sphere (N)

F_G the downward force of gravity acting on the particles (N)

f_M the correction factor for materials of construction

f_P the correction factor for design pressure

f_T the correction factor for design temperature

g the acceleration of gravity

GSD Geometric Standard Deviation

GSD_1 Geometric Standard Deviation of particle that enter to the first cyclone

GSD_2 Geometric Standard Deviation of particle that enter to the second cyclone

H the overall height of the cyclone (m)

h the cylinder height of the cyclone (m)

H_0 the ratio of overall height of the cyclone

h_0 the ratio of cylinder height of the cyclone

H_{CS} the heigt of CS

j constant

K_x the vortex finder entrance factor

$K_{(1D3D)}$ cut-size diameter correction factor for cyclone 1D3D

$K_{(2D2D)}$ cut-size diameter correction factor for cyclone 2D2D

$K_{(1D3D)_1}$ cut-size diameter correction factor for the first cyclone 1D3D

$K_{(1D3D)_2}$ cut-size diameter correction factor for the second cyclone 1D3D

$K_{(2D2D)_1}$ cut-size diameter correction factor for the first cyclone 2D2D

$K_{(2D2D)_2}$ cut-size diameter correction factor for the second cyclone 2D2D

m_p the mass of the particle

m_{p1_k} the mass of particle that goes through the first cyclone of each level

m_{p1} the mass of particle that enter to the first cyclone in series arrangement

m_{p2_k} the mass of particle that goes through the second cyclone of each level

m_{p2} the mass of particle that enter to the second cyclone in series arrangement

m_{p3} the mass of particle that enter to the third cyclone in series arrangement

$m_{p_{out}}$ the mass of the emission of the cyclone system

MMD Mass Median Diameter

MMD_1 Mass Median Diameter of particle that enter to the first cyclone

MMD_2 Mass Median Diameter of particle that enter to the second cyclone

N number of cyclones

N_H the number inlet velocity heads of the gas

N_i the number of spiral turns of particle inside the cyclone

N_K number of level of the cyclone arrangement

N_p number of parallel cyclone lines

N_p^U the upper bound of number of parallel lines

N_S number of stage of the arrangement

N_s number of series cyclone in each parallel line

$N_{i_{(1D3D)}}$ the number of spiral turns of particle inside the cyclone 1D3D

$N_{i_{(2D2D)}}$ the number of spiral turns of particle inside the cyclone 2D2D

N_{p_k} the number of parallel lines on level k

$N_{p_k}^U$ the upper bound of number parallel lines on level k

Q the inlet flow rate to cyclone

q term in Stairmands pressure drop model

Q_k the flow rate through level k

Q_k^U	the upper limit of the total flow rate through level k
Q_p	the flow rate of each cyclone in parallel arrangement
Q_t	the total flow rate through the arrangement
Q_{p_k}	the flow rate through parallel cyclone on level k
$Q_{p_k}^U$	the upper limit of the parallel flow rate through level k
R	the cyclone radius
r	the radius of particle (m)
R_e	the gas outlet or vortex finder radius
S	the gas outlet length (m)
S_0	the ratio of gas outlet length
t_w	the time worked per year
v_θ	the tangential velocity of particle (m/s)
$v_{\theta CS}$	the tangential velocity in CS
$v_{\theta max}$	the maximum tangential velocity, that occurs at the edge of the control surface CS
v_i	the gas inlet velocity (m)
v_i^L	the lower bound of inlet velocity
v_i^U	the upper bound of inlet velocity
v_{rCS}	the uniform radial gas velocity in the surface of CS (Control Surface / Cylindrical Surface)
v_s	the saltation velocity

v_t	the terminal velocity of particle (m/s)
v_x	the average axial velocity through the vortex finder
v_{1D2D}	the inlet velocity of 1D2D cyclone
v_{1D3D}	the inlet velocity of 1D3D cyclone
v_{2D2D}	the inlet velocity of 2D2D cyclone
v_{θ_w}	the velocity in the vicinity of the wall
v_{i_k}	the inlet velocity of gas through level k
$v_{i_k}^L$	the lower bound of inlet velocity on level k
$v_{i_k}^U$	the upper bound of inlet velocity on level k
v_{i_p}	the inlet velocity of cyclone in parallel arrangement
v_{i_s}	the inlet velocity of cyclone in series arrangement
$v_{i_{max}}$	the maximum inlet velocity
x_k	the fraction of total flow through level k
Y	the number of years over which depreciation occurs
z	binary variable
z_k	binary variable of level k

Chapter 1

Introduction

1.1 Research capabilities

Most of the initial cyclones were used in agricultural processing to collect dust created from mills as a result of processed grains and wood products. In the decades that have followed, the gas solid cyclone became one of the most widely used of all types of industrial gas-cleaning devices. Cyclones are frequently used as finishing collectors in cases wherein large particles have to be caught. Designing optimum cyclone arrangements became more essential with the growing concern of the environmental effects of particulate pollution. A single cyclone can usually give sufficient gas-solid separation for a particular process or application. However, solids separation task can sometimes be enhanced by placing multiple cyclones either in series or parallel. Cyclones in series are typically necessary for most processes to minimize the loss of expensive solid reactant or catalyst. Meanwhile, several cyclones are placed in parallel when extremely high centrifugal forces are required. Mathematical programming (i.e., linear or nonlinear programming and mixed integer programming) can be used to determine the optimum cyclone arrangement in order to minimize particulate emissions. Development of these mathematical models can be challenging when the operation cost and the capital cost of the cyclone arrangement

are taken into account. The capital cost is proportional to diameter of the cyclone and the number of cyclone. Meanwhile, the operating cost is proportional to inlet flow rate to the cyclone and the cyclone pressure drop. Installing the cyclones in parallel, would lead to higher capital cost. On the other hand, the cyclones in series arrangement would bring to higher operating cost instead. Therefore, the models must have a capability to optimize the number of cyclones and dimensions when determining the optimum cyclone arrangement (in series and/or in parallel) with the minimum total cost.

In this study, the mathematical modelling will be developed to determine the optimum cyclone arrangement for two cases; nonlinear programming optimization of series and parallel cyclone arrangement and MINLP optimization of cyclones arrangement in parallel-series for 1D3D, 2D2D, and 1D2D cyclones.

All mathematical models are implemented in the General Algebraic Modeling System (GAMS) software [86]. GAMS is a high-level modeling system for mathematical programming and optimization. The package has an enormous number of features and options to support the most sophisticated mathematical programming and econometric applications.

The optimization models which are developed can be implemented to control the emissions of particulate matter in plants that operate cyclones as their dedusting system. Moreover, the optimization of cyclone arrangement in NPK (Nitrogen, Phosphorus, and Potassium) fertilizer plant and paper mill plant will be presented.

1.2   Overview on cyclones

Cyclone is a device that separates the dust particles from the gas stream as a result of centrifugal forces acting on the particles in the swirling gas stream. A swirling motion is created by the tangential injection of the gas that enter the cyclone. The centrifugal force drives the dust to the cyclone wall. After hitting the wall, the particles fall to the bottom dust outlet and are collected. The most common types of centrifugal cyclone in use recently are single-cyclone separators and multiple-cyclone separators. Single-cyclone

separator create a dual vortex to separate dust from the gas. The main vortex spirals downward and carries most of the heavier particles. The inner vortex, created near the bottom of the cyclone, spirals upward and carries finer dust particles. Multiple-cyclone separators consist of a number of small-diameter cyclones, operating in parallel or in series. It is usually used when the solids concentration is high and the emission from just one separator stage would be too high.

In general, cyclones are made in a variety of configurations. The most common geometry of a reverse-flow cyclone is determined by the following dimensions as shown in Figure 1.1:

1. a = the inlet height (m)

2. b = the inlet width (m)

3. B = the dust outlet diameter (m)

4. D = the diameter of the cyclone (m)

5. D_e = the gas outlet or vortex finder diameter (m)

6. S = the gas outlet length (m)

7. h = the cylinder height of the cyclone (m)

8. H = the overall height of the cyclone (m)
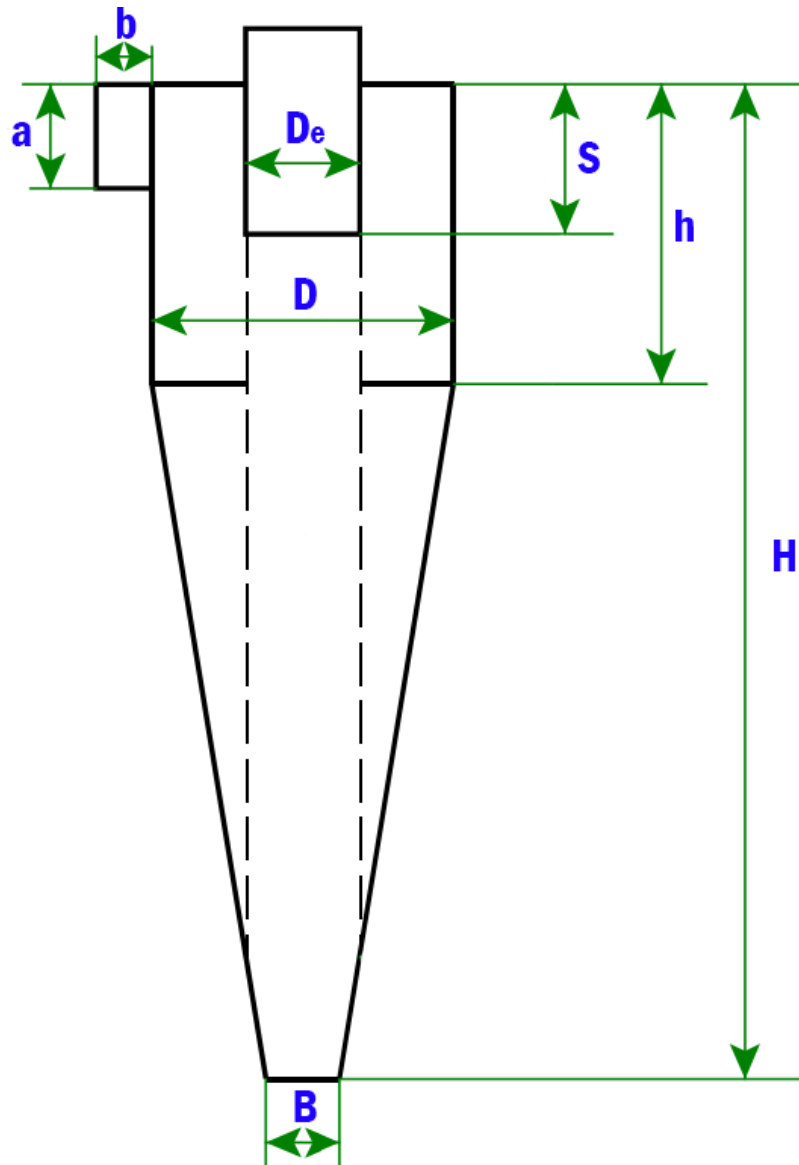
Figure 1.1: Schematic diagram of a reverse-flow cyclone

In this study, a general rule has been employed for representing cyclone configurations. If cyclone configuration is named nDmD, the height of the cylinder (h) and the cone section (H - h) of the cyclone would be equal to (n x D) and (m x D), respectively. For instance,

2D3D cyclone means a cyclone with cylinder height and cone height of two and three times of cyclones diameter. The configurations of cyclones that are considered in this work are 1D3D [36], 2D2D [94], and 1D2D [96]. All the mentioned configurations are listed in Table 1.1. It should be noted that if the values of both H_0 and h_0 are set for any configuration of the cyclone, the rest of the ratios will be known for that specific configuration.

Ratio	Cyclone 1D3D	Cyclone 2D2D	Cyclone 1D2D
$a_0 = \frac{a}{D}$	0.5	0.5	0.5
$b_0 = \frac{b}{D}$	0.25	0.25	0.25
$S_0 = \frac{S}{D}$	0.125	0.125	0.625
$D_{e0} = \frac{D_e}{D}$	0.5	0.5	0.625
$H_0 = \frac{H}{D}$	4	4	3
$h_0 = \frac{h}{D}$	1	2	1
$B_0 = \frac{B}{D}$	0.25	0.25	0.5

Table 1.1: Cyclone configuration ratio

1.3 Research objectives

The design of using a single cyclone connected to each particulate matter source device is common in many industrial applications. In spite of the fact that each cyclone has been designed with excellent performance to handle separation of particles, there are many situations wherein a single cyclone is inadequate for the particle separation task. In such

situations, it is often feasible to use multiple units either in series or in parallel or both. Therefore, the main objectives of this research are as follows:

1. To observe the feasibility to use multiple units of cyclone in actual NPK fertilizer plant.

2. To develop a MINLP (Mixed Integer Nonlinear Programming) optimization model in order to select the best arrangement of cyclones in parallel-series.

1.4   Outline of the thesis

This thesis is organized in five chapters as follows:

Chapter 2 presents the literature review on the key subjects covered in this work. The studies relevant to the optimization of cyclone arrangement are reviewed. Several studies have been conducted in experimental, theoretical, and computational research on cyclones are also summarized in this chapter.

Chapter 3 present the nonlinear programming optimization of series and parallel cyclone arrangement. The key idea in this work is to observe the feasibility to use multiple units of cyclones in order to reduce the emissions in the actual Nitrogen, Phosphorus, and Potassium (NPK) granulation plant. Furthermore, the best cyclone configurations and the optimum arrangement whether in series or parallel are obtained by using GAMS software.

Chapter 4 presents a novel optimization of parallel-series cyclone arrangement. The key novelties of the proposed method include the use of a mixed integer nonlinear programming (MINLP) implemented in GAMS software to find the best cyclone arrangement with the optimal number of cyclones and dimensions from several combinations of 1D3D and 2D2D cyclone arranged in parallel-series. A case study with a total flow rate of 165 m^3/s of a stream to be processed in a paper mill is used to test the proposed method.

Chapter 5 summarizes the key research outcomes of the research avenues that can be further explored in this area.

Chapter 2

Literature Review

2.1 Introduction

Cyclones are commonly used air pollution abatement devices for separating particulate matter (PM) from air streams in industrial processes. Compared to other abatement systems, cyclones have low initial costs, maintenance requirements, and energy consumption. There are basically two modeling approaches for evaluating the performance of a cyclone, i.e, the equilibrium-orbit models and time-of-flight models. These models are based on a force balance on a particle that is rotating in a cylindrical surface (CS) at radius $R_e = \frac{1}{2}D_e$. Figure 2.1 (a) illustrates the concept of the equilibrium-orbit models. CS is formed by continuing the vortex finder wall to the bottom of the cyclone. Since there are two forces in balance which are the centrifugal force and the inward drag caused by the gas flowing through, large particles are centrifuged out from the cyclone wall and small particles are dragged in and move out through the vortex tube. The particle size for which the two forces balance (the size that orbits in equilibrium in CS) is taken as the d_p or the cut-size diameter. As such, it is the particle size that stands a 50-50 chance of being captured. This particle size is very important in measuring the separation capability of the cyclone. Figure 2.1 (b) illustrates the other modeling approach, i.e., time-of-flight modeling. In this model,

the particle's migration to the wall is considered, neglecting the inward gas velocity. The total path length for a particle swirling close to the wall (assumed cylindrical) is: $\pi D N_i$, where N_i is the number of spiral turns the particle takes on its way toward the bottom of the cyclone. The smallest particle size that can traverse the entire width of the inlet jet before reaching the bottom of the cyclone as a critical particle size is considered as the d_p. It can be seen that the time-of-flight modeling concept is entirely different in nature from the equilibrium-orbit concept. Although the time-of-flight models predict somewhat larger cut sizes than the equilibrium-orbit models, the time-of-flight concept is found very consistent with what is seen in CFD simulations. and it can become the most promising for formulating models for the performance of cylindrical cyclones [55]. In addition, all the equations used in this work will be derived from the time-of-flight model.
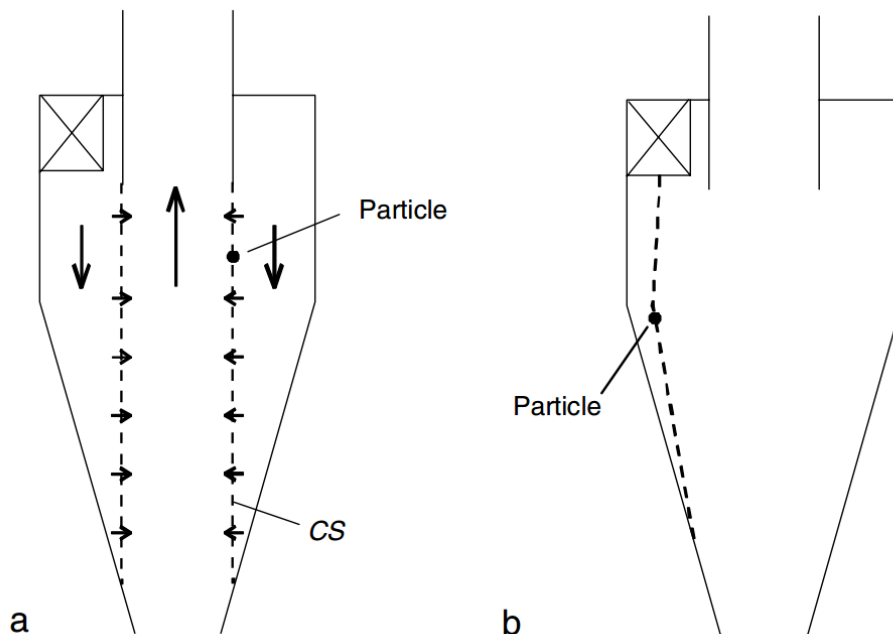
Figure 2.1: Sketches of the concept of: a. the equilibrium-orbit models, and b. the time-of-flight models [55]

There are three main approaches on the study of cyclone performance in the literature:

- Mathematical models, which can be classified into: theoretical and semi-empirical models, and statistical models

- Experimental measurements

- Computational fluid dynamics (CFD) simulations

Recently, a novel mathematical model of multiple cyclone arrangement has been developed. In addition, GAMS software also employed in the optimization [86] in order to deliver the best results and reliable solutions.

2.2   Mathematical models

The theoretical or semi-empirical models of cyclones have been developed to acquire more desirable understanding and prediction of cyclones' performances to improve computation, e.g., Alexander [3], First [28], Barth [6], Casal and Martinez-Benet [11], Stairmand [101], Karagoz and Avci [59], Zhao [123], Avci and Karagoz [5], and Chen and Shi [12]. The majority of these models have been derived by using physical descriptions and mathematical equations. These equations depend mainly on the characteristics of gas and particle motion within the cyclone and energy dissipation mechanisms of cyclones. Over the years, interest in particle collection and pressure drop of the cyclone theories has steadily increased. The accuracy of the performance equations depends upon how well the assumptions made in their development reflect the actual operating conditions within the cyclone. The most widely used mathematical models of cyclone prediction performance are:

- Barth model [6]

- Stairmand model [101]

- Casal and Martinez-Benet model [11]

- Shepherd and Lapple model [94]

- The Muschelknautz method of modeling (MM) [55]

- Ramachandran model [82]

- Iozia and Leith model [57]

- Rietema model [85]

Some simplifying assumptions are common to all these models. They can be considered as offering a good compromise between accurate prediction and simplification of the equations:

- The particles are spherical

- The radial velocity of the gas equals zero

- The radial force on the particle is given by Stokes law

2.2.1 Estimation of the cut-size diameter

- Barth model
  Barth [6] proposed a simple model based on force balance (classified as one of the equilibrium-orbit models [55]). This model considers the imaginary cylindrical surface (CS) that is formed by continuing the vortex finder wall to the bottom of the cyclone, see Figure 2.1. Here, all the gas velocity components are assumed constant over CS for the computation of the equilibrium-orbit size. The Barth model for theoretical cut-size diameter is given as below:

$$d_p = \left[\frac{9 \, \mu \, D_e \, v_{rCS}}{\rho_p \, v_{\theta CS}^2} \right]^{\frac{1}{2}} \tag{2.1}$$

where v_{rCS} is the uniform radial gas velocity in the surface of CS given by:

$$v_{rCS} = \frac{Q}{\pi \, D_e \, H_{CS}} \tag{2.2}$$

H_{CS} can be obtained by the following expression:

$$H_{CS} = \frac{(R - Re)\,(H - h)}{R - (B/2)} + (h - S) \qquad\qquad \text{if } B > De \qquad (2.3)$$

$$= (H - S) \qquad\qquad\qquad\qquad \text{if } B \leq De \qquad (2.4)$$

- The Muschelknautz method of modeling (MM)

  The cut-size diameter is analogous to the screen openings of an ordinary sieve or screen [55]. In lightly loading cyclones, the cut-size exercises a controlling influence on the cyclone's separation performance that determines the horizontal position of the cyclone grade-efficiency curve (fraction collected versus particle size). For low mass loading, the cut-off diameter can be estimated in MM using the following equation:

$$d_p = \left[\frac{9\,\mu\,(0.9\,Q)}{\pi\,(\rho_p - \rho)\,v_{\theta CS}^2\,(H - S)} \right]^{\frac{1}{2}} \qquad (2.5)$$

- Iozia and Leith model

  The Iozia and Leith model [57] is similar to the model of Barth [6] as it is also based on the equilibrium-orbit theory. Iozia and Leith [57] gave the following expression for the cut-size diameter:

$$d_p = \left[\frac{9\,\mu\,Q}{\pi\,H_{CS}\,\rho_p\,v_{\theta max}^2} \right]^{\frac{1}{2}} \qquad (2.6)$$

  where:

  $H_{CS} \triangleq$ the core height (height of the control surface of Barths model)

  $v_{\theta max} \triangleq$ the maximum tangential velocity, that occurs at the edge of the control surface CS

  The value of the core diameter D_{CS} and the tangential velocity at the core edge $v_{\theta max}$ are calculated from regression of experimental data using the following equations:

$$v_{\theta max} = 6.1\,v_i \left(\frac{ab}{D^2} \right)^{0.61} \left(\frac{D_e}{D} \right)^{-0.74} \left(\frac{H}{D} \right)^{-0.33} \qquad (2.7)$$

$$D_{CS} = 0.52\,D \left(\frac{ab}{D^2} \right)^{-0.25} \left(\frac{D_e}{D} \right)^{1.53} \qquad (2.8)$$

11

- Rietema model

  The Rietema model relates the cut-size diameter to pressure drop. Hence, the pressure drop needs to be predicted to use the model. The following expression is used to calculate the cut-size diameter:

$$d_p = \left[\frac{\mu \, \rho \, Q}{H \, (\rho_p - \rho) \, \Delta P} \right]^{\frac{1}{2}} \tag{2.9}$$

  A good pressure drop model for this purpose is that of Shepherd and Lapple [95]. The pressure drop (ΔP) based on the Shepherd and Lapple model is expressed in term of the number inlet velocity heads of the gas (N_H):

$$\Delta P = \frac{1}{2} \rho v_i^2 N_H \tag{2.10}$$

  where:

$$N_H = \frac{16ab}{D_e^2} \tag{2.11}$$

2.2.2 Estimation of the pressure drop

- Barth model

  Barth subdivided the pressure drop into three contributions:

  1. the inlet losses (Barth assumed that this loss could be effectively avoided by good design)

  2. the losses in the cyclone body

  3. the losses in the vortex finder

12

The total pressure drop is the summation of the pressure drop in the cyclone body ΔP_{body} and the pressure drop in the vortex finder ΔP_x.

$$\Delta P_{body} = \frac{1}{2}\rho v_x^2 \left(\frac{D_e}{D}\right) \left[\frac{1}{\left(\frac{v_x}{v_{\theta CS}} - \frac{H-S}{0.5D_e}f\right)^2} - \left(\frac{v_{\theta CS}}{v_x}\right)^2\right] \tag{2.12}$$

$$\Delta P_x = \frac{1}{2}\rho v_x^2 \left[\left(\frac{v_{\theta CS}}{v_x}\right)^2 + K_x \left(\frac{v_{\theta CS}}{v_x}\right)^{\frac{4}{3}}\right] \tag{2.13}$$

where:

$$f \triangleq \text{the friction factor}$$

$$K_x \triangleq \text{the vortex finder entrance factor}$$

$$(K_x = 3.41 \text{ for rounded edge and } K_x = 4.4 \text{ for sharp edge})$$

- The Muschelknautz method of modeling (MM)

  According to the MM model, the pressure loss across a cyclone (ΔP) occurs, primarily, as a result of friction with the walls (ΔP_{body}) and irreversible losses within the vortex core (ΔP_x).

$$\Delta P_{body} = f\frac{A_R}{0.9Q}\frac{\rho}{2}(v_{\theta CS}v_{\theta w})^{1.5} \tag{2.14}$$

$$\Delta P_x = \left[2 + \left(\frac{v_{\theta CS}}{v_x}\right)^2 + 3\left(\frac{v_{\theta CS}}{v_x}\right)^{4/3}\right]\frac{1}{2}\rho v_x^2 \tag{2.15}$$

where:

$$A_R \triangleq \text{the total inside area of the cyclone contributing to frictional drag}$$

$$v_{\theta w} \triangleq \text{the velocity in the vicinity of the wall}$$

$$v_x \triangleq \text{the average axial velocity through the vortex finder}$$

13

- Several expressions of empirical model have been developed to predict the cyclone pressure drop. Most of the models express ΔP in terms of the number of inlet velocity heads of the gas, N_H.

$$\Delta P = \frac{1}{2}\rho v_i^2 N_H \tag{2.16}$$

The value of N_H is usually a constant for geometrically similar cyclones of different diameters. The most widely used equations are mentioned below:

- Stairmand model
  Stairmand [101] estimated the pressure drop as entrance and exit losses combined with the static pressure loss in the swirl.

$$N_H = 1 + 2q^2\left(\frac{2(D-b)}{D_e} - 1\right) + 2\left(\frac{4ab}{\pi D_e^2}\right)^2 \tag{2.17}$$

- Sphered and Lapple model [95]

$$N_H = \frac{16ab}{D_e^2} \tag{2.18}$$

- Casal and Martinez-Benet model [11]

$$N_H = 3.33 + 11.3\left(\frac{ab}{D_e^2}\right)^2 \tag{2.19}$$

- Ramachandran model
  The Ramachandran et al. [82] model was developed through a statistical analysis of pressure drop data for ninety-eight cyclone designs.

$$N_H = 20\left[\frac{ab}{D_e^2}\right]\left[\frac{\frac{S}{D}}{\frac{H}{D}\frac{h}{D}\frac{B}{D}}\right]^{\frac{1}{3}} \tag{2.20}$$

14

2.3 Experimental methods

There are numerous experimental measurements performed on the cyclone separators. Some of the studies measured the pressure drop and collection efficiency. For example, Dirgo and Leith [17] measured the collection efficiency and pressure drop for the Stairmand high efficiency cyclone at different flow rates. Hoffmann et al. [54] investigated the effect of cyclone length on the separation efficiency and the pressure drop experimentally and theoretically by varying the length of the cylindrical segment of a cylinder-oncone cyclone. They found for cyclone lengths from 2.65 to 6.15 cyclone diameters, a marked improvement in cyclone performance is achieved with increasing length up to 5.5 cyclone diameters; beyond this length the separation efficiency was dramatically reduced. Other experimental results on cyclones can also found in [119, 100, 76, 60, 52, 53, 16]. The majority of these models have focused on the development of single cyclones. Other researchers established experiments to observe the performance of multi cyclone arrangements. Gillum et al. [40] investigated the arrangement of an existing 2D2D cyclone connected to 2D2D cyclone for the first test and to a 1D3D cyclone for the second test. Gillum and Hughs [39] held an experiment with the variation of the inlet velocity ranged from 11.8 to 18.3 m/s through two cyclones in series, 2D2D primary and 2D2D or 1D3D secondary. Columbus [15] also studied a 2D2D primary cyclone in series with a 1D3D secondary cyclone in capturing particulate matters (PM) emitted from a seed cotton separator. Whitelock and Buser [118] evaluated the effectiveness of up to four 1D3D cyclones in series on heavy loading of particulate air streams (236 g/m^3). These studies showed that the series arrangement had a significant improvement in cyclone overall efficiency compared to a single cyclone. However, having the two cyclones in series appeared to be the best choice because of the use of three or four cyclones in series only slightly increased the overall efficiency along with a significant increase in the pressure drop across all cyclones [118].

2.4 Computational fluid dynamics (CFD) simulations

The CFD technique became a widely used approach for the flow simulation and performance estimation of cyclone separators. The CFD modeling approach is able to predict the features of the cyclone flow field in great details, which provide a better understanding of the fluid dynamics in cyclone separators [43]. The pressure drop predicted by CFD was also found in an excellent agreement with measured data. Moreover, Gimbun et al. [41] successfully applied CFD to predict and to evaluate the effects of temperature and inlet velocity on the pressure drop of gas cyclones. This makes the CFD methods represent a reliable and cost-effective route for geometry optimization in comparison with the experimental approach. However, CFD is still more expensive in comparison with the simplified mathematical modeling approach. The main reasons behind the cost of the CFD approach with respect to the mathematical methods are:

- The license cost of the grid generator, solver and post processor

- The running cost especially for unsteady state simulations which need also parallel processing

- The CFD process requires expert intervention by an expert researcher at every stage (mesh generation, solver settings and post processing)

- CFD results always need validation with experimental results, and perform the same simulation on different grids to be sure that the obtained results are grid independent.

2.5 Mathematical programming models

Mathematical programming provides a general modeling framework for optimization that finds many interesting applications in chemical engineering. For example, linear programming (LP) has been extensively used for refinery scheduling and batch production planning

problems (e.g., Symonds [105], Mauderli and Rippin [73]). Mixed integer linear programming (MILP) has been used for the synthesis of process systems with simplified models (e.g., Grossmann and Santibanez [50], Papoulias and Grossmann [74]), and for batch scheduling (e.g., Rich and Prokopakis [84], Ku and Karimi [66], Kondili et al. [64], Shah et al. [93], Pinto and Grossmann [79]). Nonlinear programming (NLP) has been used for separation process design and optimization (e.g., Sargent and Gaminibandara [91], Kumar and Lucia [67]). Mixed-integer nonlinear programming (MINLP) has been used for process synthesis (e.g., Grossmann [44, 48, 45, 46], Duran and Grossmann [21], Kocis and Grossmann [62, 63], Floudas and Paules [32], Kravanja and Grossmann [65], Grossmann and Kravanja [49]), distillation design (e.g., Viswanathan and Grossmann [109, 110], Ciric and Gu [13]), process scheduling (e.g., Sahinidis and Grossmann [90], Tsirukis et al. [106], Pinto and Grossmann [78]), process control strategy (e.g., [92]), and pump configurations (e.g., Pettersson and Westerlund [77], Westerlund et al. [117]). The application of these mathematical programming tools has provided useful results. Moreover, NLP and MINLP techniques are applied in the present work for multiple cyclone arrangement problems.

2.5.1   Nonlinear Programming (NLP) models

The nonlinear programming problem can be defined as follows:

$$
\begin{aligned}
Min \quad & f(x) \\
s.t. \quad & h(x) \ = \ 0 \\
& g(x) \ \leq \ 0
\end{aligned}
$$

Sufficient conditions that guarantee global optimality are that f(x) convex, h(x) linear, and g(x) convex. These nonlinear programming models and techniques are frequently used in the optimization of process systems in chemical engineering. However, these NLP models often include non-convex functions (e.g., f(x) and g(x) concave, h(x) nonlinear) that give rise to multiple suboptimal solutions and non-optimal stationary points. Consequently, a solution obtained for a non-convex model with a standard optimization algorithm

17

(e.g., generalized reduced gradient, successive quadratic programming) which is commonly rigorous for convex problems, is strongly dependent on the starting point. Moreover, linearizations of non-convex constraints of feasible problems can define infeasible regions or produce indefinite Hessian matrices that often cause the failure of standard local optimization techniques [70].

The problem of determining a global optimum solution for non-convex NLP problems is generally very difficult. No algorithm can solve a general and smooth global optimization problem with certainty in a finite number of steps, unless some kind of tolerance for the precision of the global minimum is pre-specified [18]. Depending on whether global optimization techniques incorporate stochastic elements or not, they are classified as stochastic or deterministic [19]. Stochastic techniques are applicable to optimization problems that do not exhibit special structures, but can not guarantee convergence to a global optimum in finite time. Deterministic global optimization techniques on the other hand are designed to converge to a global optimum solution with certainty or to prove that such a point does not exists. To provide this kind of guarantee, deterministic techniques make a number of specific assumptions and restrict their applicability to specific classes of problems. Excellent surveys on deterministic techniques and more references to the literature can be found in Horst [56].

The issue of non-convex optimization and the concern for finding global optimal solutions have been present in the chemical engineering literature since the pioneering work by Stephanopoulos and Westerberg [102]. A non-deterministic approach for the solution of non-convex models in chemical engineering includes the works by Kocis and Grossmann [63], Floudas et al. [30], Floudas and Ciric [31], Viswanathan and Grossmann [108], Floudas and Aggarwal [34]. Deterministic algorithms for the global optimization of certain classes of NLP models in chemical engineering can be found in the following citations: the GOP algorithm by Floudas and Visweswaran [33, 35], the branch and bound algorithm for factorable programs by Swaney [104] and Epperly and Swaney [24], the global optimization algorithm for rationally constrained rational programming problems by Manousiouthakis and Sourlas [71], the interval global optimization algorithm by Vaidyanathan and El-Halwagi [107], the

branch and bound algorithm for programs with linear fractional and bilinear terms by Quesada and Grossmann [81], the branch and reduce algorithm by Ryoo and Sahinidis [88, 89], the αBB algorithm by Androulakis et al. [4], and the reformulation spatial branch and bound algorithm for general process models by Smith and Pantelides [98].

2.5.2 Mixed Integer Nonlinear Programming (MINLP) models

A mixed integer program (MIP) is an optimization problem that involves continuous as well as integer variables. The most frequent case of MIP is the one in which the integer variables are restricted to be of the 0 - 1 type (binary variables):

$$
\begin{aligned}
Min \quad & f(x, y) \\
s.t. \quad & h(x, y) \;=\; 0 \\
& g(x, y) \;\leq\; 0 \\
& x \;\epsilon\; R^n \;\;,\;\; y \;\epsilon\; \{0, 1\}^m
\end{aligned}
$$

A MIP is said to be linear (MLP) if the objective function and the constraints that define the feasible set are linear, otherwise the MIP is said to be nonlinear (MINLP). For the case of an MILP the LP relaxation is convex. Thus, global optimality can be guaranteed with a branch and bound algorithm since rigorous lower bounds are predicted. When the values of all the integer variables in a MINLP are fixed, a NLP problem in the continuous subspace is obtained. Both, MILPs and MINLPs are non-convex programs since they have disconnected feasible regions due to their discrete nature. Hence, non-convexities may also arise in the feasible subspace for the continuous variables (e.g., f(x,y), g(x,y) non-convex for fixed y, h(x,y) nonlinear for fixed y). A MINLP model is said to be non-convex if the relaxation of the integrality condition yields a non-convex NLP problem.

There has been recently an increased interest in the development of mixed integer nonlinear programming (MINLP) in the area of engineering design, planning, scheduling and marketing. Several techniques for the solution of MINLP models are Generalized

Benders Decomposition, GBD (Geoffrion [37]), the branch and bound method (Gupta and Ravindran [51]), Outer Approximation / Equality-Relaxation Method OA/ER (Duran and Grossmann [22], Kocis and Grossmann [62], Fletcher and Leyffer [29]), the LP/NLP based branch and bound technique (Quesada and Grossmann [80]), and the extended cutting plane method (Westerlund and Pettersson [116]). Detailed descriptions of these techniques and extensive references on the subject can be found in Grossmann and Kravanja [49].

It is well known that, when applied to non-convex MINLP models, these techniques might get trapped at suboptimal solutions, or even worse, they may fail to obtain a feasible point. Viswanathan and Grossmann [108] proposed a heuristic strategy that aims at reducing the effect of non-convexities. The proposed model combined Outer Approximation / Equality-Relaxation (OA/ER) method with an Augmented Penalty (AP) function. The proposed algorithm has as main features that it starts with the solution of the NLP relaxation problem, and that it features an MILP master problem with an augmented penalty function that allows violations of linearizations of the nonlinear functions. This scheme provides a direct way of handling non-convexities which are often present in engineering design problems. The main steps in the proposed AP/OA/ER algorithm are as follows:

- Step 1:
  Solve the relaxed NLP problem in (1) to determine a KKT point (x^0, y^0). If y^0 is an integer, the solution is found, stop. Otherwise, set K = 0, $z^{OLD} = +\infty$, and go to Step 2.

- Step 2:
  Set up the MILP master problem and solve to find the integer vector y^{K+1}.

- Step 3:
  Solve the NLP subproblem $[P(y^{K+1})]$ to determine the KKT point (x^{K+1}, y^{K+1}) with objective value z^{K+1}. If the NLP is infeasible set FLAG = 0. If the NLP is feasible set $z^{NEW} = z^{K+1}$, FLAG = 1.

- Step 4:

(a) If FLAG = 1, determine if $z^{NEW} > z^{OLD}$; if satisfied, stop. The optimal solution is z^{OLD}. Otherwise, set $z^{OLD} = z^{NEW}$, set K = K + 1 and return to Step 2 by adding the corresponding linearization and integer cut.

(b) If FLAG = 0, set K = K + 1 and return to Step 2 by adding the integer cut.

It should be noted that the above algorithm will terminate in one iteration if an integer solution is found in Step 1, or else it will terminate after three or more iterations when the termination condition in Step 4 (a) is satisfied. Note that in the latter case, N iterations imply the solution of N NLP subproblems, and N-1 MILP subproblems. Also, it should be noted that since at each iteration K ≥ 1, an integer cut is added to the MILP master problem in Step 2 (even for the case of infeasible NLP subproblems), the algorithm cannot cycle and return to an integer point that has been previously examined. Finally, if convexity of the MINLP can be established a priori, the termination criterion in Step 4 can be replaced by the use of the lower bound predicted by the MILP master problem as in the OA/ER algorithm.

It is also important to note that although the proposed algorithm has provisions for trying to overcome the effect of non-convexities, it can fail to find the global optimum mainly for the two following reasons. Firstly, if the NLP relaxation has multiple local solutions with integer points, then clearly the algorithm can converge to a suboptimal point. Secondly, if the NLP subproblem for fixed binary values has different local optima, the algorithm may be trapped into a local solution. Despite these limitations, the numerical performance, which has been tested on a variety of applications has shown that the computational requirements of this method are quite reasonable while providing a high degree of reliability for finding global optimum solutions. The proposed algorithm by Viswanathan and Grossmann [108] has been implemented in DICOPT [25] as part of the solver that runs under GAMS software [86] which is used to solve the multiple cyclone arrangement problems in the present work.

Chapter 3

Nonlinear programming optimization of series and parallel cyclone arrangement of NPK fertilizer plants

This chapter presents a nonlinear programming optimization to address the optimal number and configuration of series and parallel cyclone arrangement in the NPK fertilizer plant. The organization of this chapter is as follows: an overview of process of actual NPK granulation fertilizer plant is given in Section 3.1. Next, Section 3.2 presents the objective of the study. The equations employed in the modeling is presented in Section 3.3. The mathematical models of parallel cyclone arrangement and series cyclone arrangement are presented in Section 3.4 and Section 3.5, respectively. The results of the optimization of three types of cyclone (i.e., 1D3D, 2D2D, and 1D2D) using parallel arrangement and series arrangement are presented in Section 3.7. Section 3.8 summarizes the methodology and work presented in this chapter. The content of this chapter has been published in Powder Technology [2] (see Appendix A).

3.1 Overview of process of actual NPK granulation fertilizer plant

The process diagram of the Nitrogen, Phosphorus, and Potassium (NPK) granulation plant under consideration is shown in Figure 3.1. The main involved unit in producing NPK fertilizer is the rotary drum granulator where the granulation process occurs. The raw materials for the granulator are clay, potassium chloride, phosphate rock powder, diammonium phosphate, urea prill, and some of the trace elements. Potassium chloride contains 60% of potassium oxide (K_2O), Phosphate rock contains 30% of phosphorus pentoxide (P_2O_5), Diammonium phosphate contains 18% of nitrogen and 46% of phosphorus pentoxide (P_2O_5), while Urea contains 46% of nitrogen. These raw materials should be discharged with certain ratios to the granulator. Next; water, steam, the recycled materials, and urea melt are charged. In addition, for maintaining the liquid phase, the steam is injected to the granulator.

In the next step, the materials leaving the granulator having moisture content in the range of 3 to 4 percent are sent to the rotary dryer number one. The outlet of the dryer is NPK materials with moisture content of about 2.5%. The NPK materials are transferred to the rotary dryer number two where the moisture content is reduced to 2%. However, the temperature of NPK leaving dryer number two is 65 °C and should be decreased to 45 °C. The temperature reduction is achieved by sending the NPK to the cooler unit. Furthermore, the NPK material is delivered to the vibrating screen where it is subjected to a screening process. The result of these processes is the generation of NPK with three different sizes namely oversize, on-size, and under-size NPK materials. The under-size NPK materials are recycled directly to the granulator. The oversize NPK ones first go to the crusher and then are recycled to the granulator. Hence, the recycled materials of the rotary granulator are the crushed material from the crusher and the undersized NPK material from the screening unit. The on-size NPK particles flow to the coating drum where extra protection against caking is added. The finished NPK product discharging

from the coating machine is lifted by the product elevator into the product hopper, where it is measured and packaged by an automatic packing machine before being sent into the warehouse.

Through the above-mentioned processes, there are several sources of pollution-emitting particulates. These particulates are released from the two types of dryers, the cooler, and the vibrating screen. To control the emissions of particulate matter, the plant operates with four cyclones. Each cyclone will be connected to each particulate matter source device (i.e., dryer 1, dryer 2, cooler, and vibrating screen).

Clay   Potassium chloride   Phosphate rock powder   Di-ammonium phosphate   Urea prill   Trace element

(metering) (metering) (metering) (metering) (metering) (metering)

Urea Granule

(metering)

Water / Liquid recycle → Granulator ← Pump ← Urea Melter

Dust

steam

vent

Scrubber No.1 ← Cyclone ← Dust ← Dryer No.1 ← Combustion Furnace ← Natural Gas / Diesel

Air

Captured dust to Granulator

Solid recycle

Cyclone ← Dust ← Dryer No.2 ← Combustion Furnace ← Natural Gas / Diesel

Air

Captured dust to Granulator

Cyclone ← Dust ← Cooling   Large Granule Crusher

Captured dust to Granulator

Granule larger than 4.5mm

Dust

Cyclone ← Screen

Captured dust to Granulator

Granule size < 2.5mm

Vent

Settling pond   Scrubber No.2   Coating Machine

Product packaging

Product

Figure 3.1: Process diagram of NPK granulation fertilizer

25

3.2 Objective of the study

Cyclone is used as a first stage to control the emissions of particulate matter in NPK granulation fertilizer plant. These particulate matters are actually the part of raw materials that can be used to produce again the NPK fertilizer by sending it to the granulator. In order to maintain a low losses in the plant, the performance of those cyclones as a dedusting system must be satisfied. Despite all the cyclones have been designed with high efficiency, high production targets may lead to decrease efficiency of the cyclone.

While the NPK fertilizer plant must be operated at its maximum capacity, an improvement of cyclone operation to maintain the low emissions should be sought. There are several options available to reach an optimum operating condition of cyclone. Each of these options has associated with a certain cost and a certain reduction capability. In this work, it is desired to observe a feasibility to use multiple units of cyclone in order to reduce the emissions. Furthermore, the best cyclone configurations and the optimum arrangement whether in series (Figure 3.3) or parallel (Figure 3.2) will be resulted from simulation using NLP model. The objective function is to minimize the total cost, including the operating cost and the capital cost. It is noted that the objective of the present study is not to compare the two types of arrangements but instead to determine the most suitable arrangement for a given fertilizer plant under study and optimize its configuration and dimensions.

3.3 The equations employed in the modeling

3.3.1 Equation for the cut-size diameter

In a gas-solid cyclone, the solid particles are mostly moving at their terminal velocity with respect to the gas. Therefore, the terminal velocity of a given solid particle decide whether the particle would be captured by the cyclone or not (i.e., escape to the atmosphere

or not). The terminal velocity is exactly analogous to that of a particle settling in the earth's gravitational field (g) under steady-state conditions. However, for a cyclone, the gravitational force is replaced by the radially directed centrifugal force [55] as shown in Eq.(3.1).

$$F_G = m_p \left(\frac{v_\theta^2}{r} \right) \tag{3.1}$$

where:

$F_G \triangleq$ the downward force of gravity acting on the particles (N)

$m_p \triangleq$ the mass of the particle (kg)

$v_\theta \triangleq$ the tangential velocity of particle (m/s)

$r \triangleq$ the radius of particle (m)

A viscous drag force is experienced when any object rises through fluid. If viscous drag force happens inside the cyclone with assumption of no slip between the fluid and the particle surface (i.e., at the surface of the particles, the velocity would be the same as the fluid one), then the Stokess drag law Eq.(3.2) can be applied for mathematical modeling [9].

$$F_d = 3\pi \mu d_p v_t \tag{3.2}$$

where:

$F_d \triangleq$ the drag force of the fluid on a sphere (N)

$d_p \triangleq$ the particle diameter (m)

$\mu \triangleq$ the dynamic viscosity (Ns/m^2)

$v_t \triangleq$ the terminal velocity of particle (m/s)

When the solid particle falls, the particle velocity increases until it reaches a velocity known as the terminal velocity. The centrifugal force quickly accelerates the particle to its terminal velocity in the radial direction. At this constant velocity, the frictional drag due to viscous forces is balanced by the gravitational force. By combining Eqs.(3.1) and (3.2), Eq.(3.3) is produced as the following:

$$v_t = \frac{2 \, m_p \, v_i^2}{3 \, \pi \, \mu \, d_p \, D} \tag{3.3}$$

where

$$v_i = v_\theta \triangleq \text{the gas inlet velocity (m)}$$
$$r = D/2 \text{ (m)}$$

Clift et al. [14] defined the mass of the particle (m_p) moving with steady terminal velocity in a gravitational field as follows in Eq.(3.4).

$$m_p = \left(\frac{\pi d_p^3}{6}\right)(\rho_p - \rho) \tag{3.4}$$

where:

$$\rho_p \triangleq \text{the particle density } (kg/m^3)$$
$$\rho \triangleq \text{the gas density } (kg/m^3)$$

Substituting Eq.(3.4) into Eq.(3.3) yields Eq.(3.5).

$$v_t = \frac{d_p^2 \, (\rho_p - \rho) \, v_i^2}{9 \, \mu \, D} \tag{3.5}$$

Moreover, Rosin et al. [87] proposed the time-flight model that compared the time required for a particle injected through the inlet of the cyclone at some radial positions to reach the cyclone wall and travel the entire width of the inlet jet before reaching the bottom of the cyclone. Assuming the inlet velocity of the particles prevail at the cyclone

28

wall, the required time for the particle to reach the bottom of the cyclone (Δt in seconds can be described as shown in Eq.(3.6).

$$\Delta t = \text{cylinderical path length / velocity} = \frac{\pi \, D \, N_i}{v_i} \tag{3.6}$$

Besides N_i is the number of spiral turns of particle inside the cyclone that can be calculated using the Lapple's expression from Eq.(3.7).

$$N_i = \frac{1}{a} \left[h + \frac{(H - h)}{2} \right] \tag{3.7}$$

The maximum radial distance traveled by any particle is the width of the inlet duct. The terminal velocity v_t that allows a particle initially at distance b away from the wall to be collected in time Δt is represented in Eq.(3.8).

$$v_t = \frac{b}{\Delta t} \tag{3.8}$$

Substituting Eqs.(3.6) to (3.8) yields Eq.(3.9).

$$v_t = \frac{b \, v_i}{\pi \, D \, N_i} \tag{3.9}$$

The smallest particle diameter that just traverses the entire width of the inlet duct to the wall and is collected can be obtained by setting the two expressions for v_t equal to each other and rearranging Eq.(3.5) with Eq.(3.9). Eq.(3.10) is obtained for the cut-size diameter.

$$d_p = \left[\frac{9 \, \mu \, b}{\pi \, N_i \, (\rho_p - \rho) \, v_i} \right]^{\frac{1}{2}} \tag{3.10}$$

The so-called cut-size diameter (d_p) is very essential as it is used in the model for the calculation of the particle collection efficiency [6]. It is assumed that the cyclone has a sharp cut at d_p (i.e., all particles' size below d_p is lost to the atmosphere and all particles' size above it is captured by the cyclone). By comparing the real efficiency found by experiments with the calculated one from the cut-size (predicted by the model), it is discovered that the results are highly accurate. This is true even when the cut-size diameter of the cyclone is far from sharp particles [55].

3.3.2   Equation for the pressure drop

The pressure drop of the cyclone in this work is expressed as the number of inlet velocity heads of the gas, N_H. The model from Casal and Martinez-Benet [11] is used to calculate the cyclone pressure drop as shown in Eq.(3.11).

$$\Delta P = \frac{1}{2} \rho \, v_i^2 \, N_H \tag{3.11}$$

where:

$$N_H = 11.3 \left(\frac{a \, b}{D_e^2} \right)^2 + 3.33 \tag{3.12}$$

3.3.3   Equation for the cost per unit of cyclone

The total cost per unit of cyclone, c_{tot} ($/s) is the summation of the operating cost (c_{opr}) and the capital cost (c_{cap}).

$$c_{tot} = c_{opr} + c_{cap} \tag{3.13}$$

The operating cost (c_{opr}) and the capital cost (c_{cap}) are calculated by Martinez-Benet and Casal [72] equations as shown in Eqs.(3.14) and (3.15) respectively.

$$c_{opr} = Q \, \Delta P \, c_e \tag{3.14}$$

where:

$$c_e \triangleq \text{the cost of utilities} \ (= \$ \ 1.5 \ \text{x} \ 10^{-8}/J \ [97])$$

$$c_{cap} = \frac{F \, e}{Y \, t_w} \, N \, D^j \tag{3.15}$$

30

where:

$F \triangleq$ the investment factor (= 4.4 [99])

$Y \triangleq$ the number of years over which depreciation occurs (= 5)

$t_w \triangleq$ the time worked per year (= 2.16 x $10^7 s/year$)

$e \triangleq$ constant (= \$ 4924.61$/m$) that is obtained from Eq.(3.16)

$j \triangleq$ constant (= 1.2) that its value depends on the equipment type [99]

$$e = \frac{C_B \; f_M \; f_P \; f_T}{D_B{}^j} \tag{3.16}$$

where the following values are obtained from Smith [99] :

$C_B \triangleq$ the known base cost for cyclone with diameter D_B (= \$ 1640)

$D_B \triangleq$ the cyclone base diameter (= 0.4 m)

$f_M \triangleq$ the correction factor for materials of construction (= 1)

$f_P \triangleq$ the correction factor for design pressure (= 1)

$f_T \triangleq$ the correction factor for design temperature (= 1)

3.4 Mathematical models of parallel cyclone arrangement

For parallel cyclone arrangement, the diameter of the cyclone (D_p, m), the inlet velocity (v_{i_p}, m/s), and the pressure drop (ΔP_p, N/m^2) are variables that will be optimized. The flow rate of each cyclone in parallel arrangement (Q_p, m3/s), the inlet velocity (v_{i_p}, m/s), and the pressure drop (ΔP_p, N/m^2) can be calculated from Eqs.(3.17 - 3.19).

$$Q_p = \frac{Q}{N} \tag{3.17}$$

$$v_{i_p} = \frac{Q_p}{a\,b} = \frac{Q}{a_0\,b_0\,D_p^2\,N} \tag{3.18}$$

$$\Delta P_p = \frac{1}{2}\rho v_{i_p}^2 N_H = \frac{1}{2}\rho \left(\frac{Q}{a_0\,b_0\,D_p^2\,N}\right)^2 N_H \tag{3.19}$$

where:

$Q \triangleq$ the total inlet volumetric flow rate of the dust leaving the NPK plant (m^3/s)

$N \triangleq$ number of cyclones

$$Q = Q_{p_1} + Q_{p_2} + \dots + Q_{p_N}$$
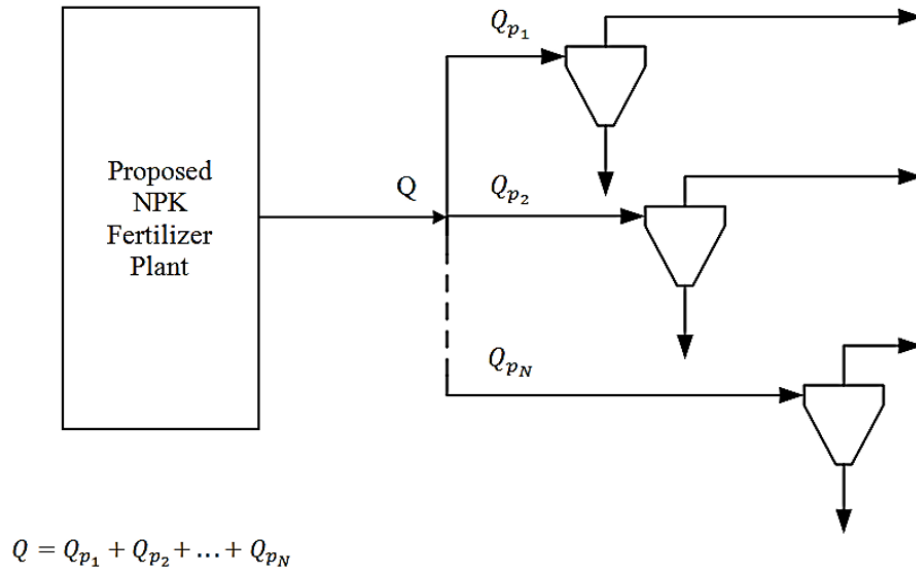
Figure 3.2: Parallel cyclone arrangement

The equation of the diameter of cyclone in parallel arrangement $(D_p$, m) is obtained by substituting Eq.(3.17) and Eq.(3.18) to Eq.(3.10), yields Eq.(3.20)

$$D_p = \left[\frac{d_p^2 \, (\rho_p - \rho) \, \pi \, N_i}{9 \, b_0^2 \, a_0 \, \mu} \frac{Q}{N} \right]^{1/3} \tag{3.20}$$

The objective function is total cost of parallel cyclone arrangement (c_{tot_p}) minimization and calculated from the following expression:

$$MIN \; c_{tot_p} = Q \, \Delta P_p \, c_e + \frac{F \, e}{Y \, t_w} \, N \, D_p^j \tag{3.21}$$

3.5 Mathematical models of series cyclone arrangement
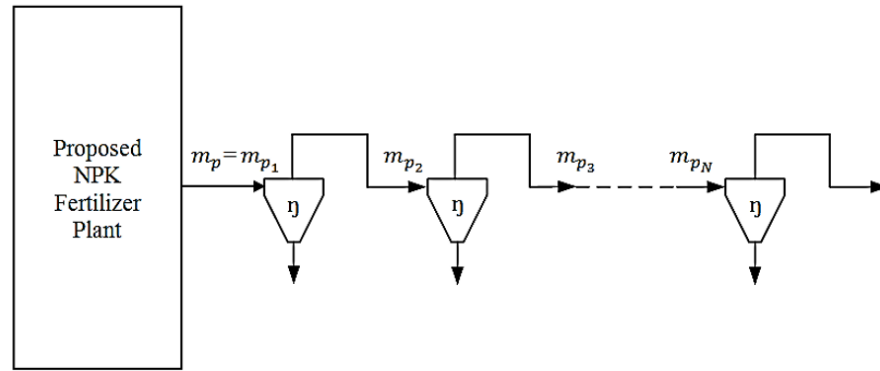
η = efficiency of the cyclone

$m_{p_2} = m_{p_1} (1 - \eta)$
$m_{p_3} = m_{p_2} (1 - \eta)$
.
.
.
$m_{p_N} = m_{p_{N-1}} (1 - \eta)$

Figure 3.3: Series cyclone arrangement

In this arrangement, the cyclones are connected in series as shown in Figure 3.3. This arrangement is set to have up to 3 cyclones with similar diameters. The diameter of the

first cyclone is calculated by using Eq.(3.20) with N = 1.

$$D_{s_1} = \left[\frac{d_{p_1}^2 \ (\rho_p - \rho) \ \pi \ N_i \ Q}{9 \ b_0^2 \ a_0 \ \mu} \right]^{1/3} \tag{3.22}$$

where D_{s_1} is the diameter of primary cyclone.

Meanwhile, as seen in the figure, the overflow mass of the particles (m_p) from the first cyclone that is charged to the next cyclone will be affected by the efficiency of the previous cyclone as indicated in Eqs.(3.23) and (3.24).

$$m_{p_1} = m_p$$

$$m_{p_2} = (1 - \eta_1) \ m_{p_1} = (1 - \eta_1) \ m_p \tag{3.23}$$

$$m_{p_3} = (1 - \eta_2) \ m_{p_2} = (1 - \eta_1)(1 - \eta_2) \ m_p \tag{3.24}$$

Based on the definition of mass particle by Clift et al. [14], Eq.(3.4) can be substituted into Eqs.(3.23) and (3.24), yields Eqs.(3.25) and (3.26).

$$m_{p_2} = (1 - \eta_1) \ \left(\frac{\pi d_{p_2}^3}{6} \right) (\rho_p - \rho) \tag{3.25}$$

$$m_{p_3} = (1 - \eta_1) \ (1 - \eta_2) \ \left(\frac{\pi d_{p_3}^3}{6} \right) (\rho_p - \rho) \tag{3.26}$$

Moreover, the equation for calculating the diameter of the second $(D_{s_2}, \ \text{m})$ and third $(D_{s_3}, \ \text{m})$ cyclone is obtained by rearranging Eqs.(3.3) and (3.9).

$$D_{s_2} = \left[\frac{2 \ m_{p_2} \ N_i \ Q}{3 \ d_{p_2} \ b_0^2 \ a_0 \ \mu} \right]^{1/3} \tag{3.27}$$

$$D_{s_3} = \left[\frac{2 \ m_{p_3} \ N_i \ Q}{3 \ d_{p_3} \ b_0^2 \ a_0 \ \mu} \right]^{1/3} \tag{3.28}$$

Substituting Eq.(3.25) into Eq.(3.27) and Eq.(3.26) into Eq.(3.28) yields Eq.(3.29) and Eq.(3.30), respectively.

$$D_{s_2} = \left[\frac{d_{p_2}^2 \ (1 - \eta_1) \ (\rho_p - \rho) \ \pi \ N_i \ Q}{9 \ b_0^2 \ a_0 \ \mu} \right]^{1/3} \tag{3.29}$$

$$D_{s_3} = \left[\frac{d_{p_3}^2 \ (1 - \eta_1)(1 - \eta_2) \ (\rho_p - \rho) \ \pi \ N_i \ Q}{9 \ b_0^2 \ a_0 \ \mu} \right]^{1/3} \tag{3.30}$$

While the flow rate for each cyclone in series arrangement would be the same, the inlet velocity (v_{i_s}, m/s) and the pressure drop (ΔP_s, N/m^2) are calculated from Eqs.(3.31 - 3.32).

$$v_{i_s} = \frac{Q}{a\,b} = \frac{Q}{a_0\,b_0\,D_s^2} \tag{3.31}$$

$$\Delta P_s = \frac{1}{2}\rho v_{i_s}^2 N_H = \frac{1}{2}\rho \left(\frac{Q}{a_0\,b_0\,D_s^2}\right)^2 N_H \tag{3.32}$$

For the series cyclone arrangement, it has two objective function problem. In this problem, the overall efficiency (η_{ov}) of the cyclone is maximized while the total cost of two series cyclones and three series cyclones are minimized. The total cost is minimized by following expression:

$$MIN\ c_{tot_s} = Q \sum_{s=1}^{N_S} \Delta P_s\ c_e + \left[\frac{F\,e}{Y\,t_w} \sum_{s=1}^{N_S} D_s^j\right] \tag{3.33}$$

$$N_S \triangleq \text{ number of stage of the arrangement}$$

The overall efficiency of the series cyclone arrangement has relationship with the efficiency of each cyclone as illustrated in Figure 3.4 and can be calculated as given in Eqs.(3.34 - 3.35).

$$mp_{out} = (1 - \eta_{ov})\, mp_{in}$$

$$mp_{out} = (1 - \eta_1)\,(1 - \eta_2)\, mp_{in}$$

$$mp_{out} = (1 - \eta_{ov})\, mp_{in}$$

$$mp_{out} = (1 - \eta_1)\,(1 - \eta_2)\,(1 - \eta_3)\, mp_{in}$$
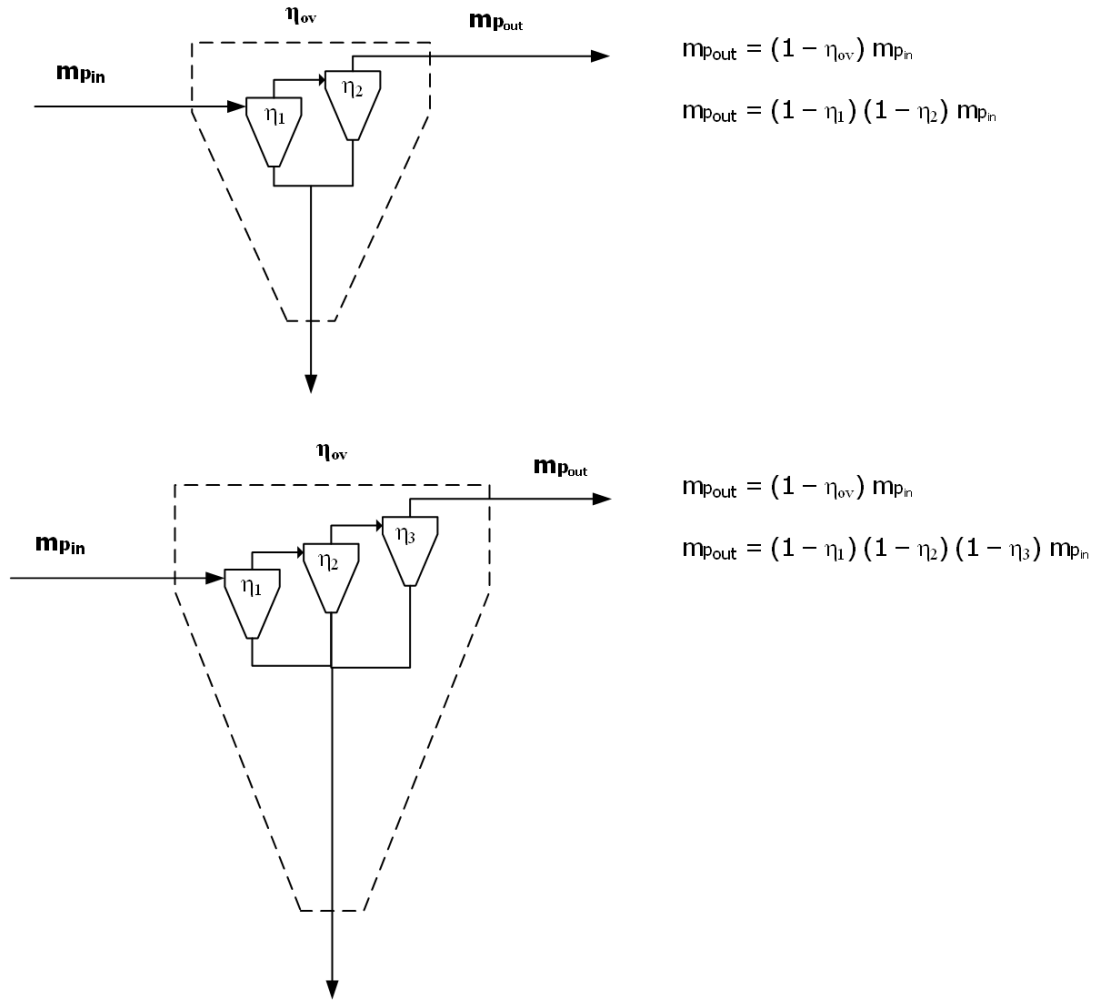
Figure 3.4: Illustration of the overall efficiency of the series cyclone arrangement

For 2 cyclones in series: $\quad \eta_{ov} = 1 - [\,(1 - \eta_1)(1 - \eta_2)\,]$ \hfill (3.34)

For 3 cyclones in series: $\quad \eta_{ov} = 1 - [\,(1 - \eta_1)(1 - \eta_2)(1 - \eta_3)\,]$ \hfill (3.35)

3.6 Constraints

The constraints of optimization model are related mainly to the pressure drop and the inlet velocity. According to Buonicore et al. [10] the pressure drop of the cyclone arrangement will have the upper bound (ΔP^L) and the lower bound (ΔP^U) and is normally accepted to be in the range as shown in Eq.(3.36).

$$500 \leq \Delta P \leq 2500 \ \ N/m^2 \tag{3.36}$$

In terms of the inlet velocity, Gimbun et al. [41] reported that for identical size and configuration of cyclone, the higher the gas inlet velocity is, the higher the efficiency would be. Nevertheless, a very high inlet velocity would decrease the collection efficiency because of increased turbulence and probability of saltation/re-entrainment of particles. Shepherd and Lapple [94] proposed the range of practicable cyclone inlet velocity which is shown in Eq.(3.37).

$$15 \leq v_i \leq 30 \ \ m/s \tag{3.37}$$

Moreover, according to Koch and Licht [61], to avoid re-entrainment of particles inside the cyclone, the inlet velocity should be less than 1.35 times the saltation velocity (v_s).

$$v_s = 4.91 \left(\frac{4g\mu(\rho_p - \rho)}{3\rho^2} \right)^{1/3} \frac{b_0^{0.4}}{(1 - b_0)^{1/3}} \ D^{0.067} \ v_i^{2/3} \tag{3.38}$$

The maximum inlet velocity of the cyclone has to be controlled in order not to exceed the maximum allowable pressure drop. The maximum value of inlet velocity must comply with its equation that is defined by Eq.(3.39).

$$v_{i_{max}} = \sqrt{\frac{2 \ \Delta P_{max}}{\rho \ N_H}} = \sqrt{\frac{2 \ (2500)}{\rho \ N_H}} \tag{3.39}$$

In summary, the lower (v_i^L) and the upper (v_i^U) constraints of the inlet velocity of the cyclone become those expressed in Eq.(3.40).

$$15 \ m/s \ \leq v_i \leq \ min \ (30 \ m/s \ , \ 1.35 v_s \ , \ v_{i_{max}}) \tag{3.40}$$

According to Smith [99], the size range of the diameter of the cyclone of which becomes the lower (D^L) and upper limit (D^U) of the diameter of the cyclone in the optimization model can be shown in Eq.(3.41).

$$0.4 \leq D \leq 3 \ m \tag{3.41}$$

In addition for the series cyclone arrangement, it is desired to maximize the overall efficiency with the following constraints:

$$0.99 \ \leq \eta_{ov} \leq \ 1 \tag{3.42}$$

where the efficiency of each cyclone based on the experimental result of multiple series cylones by Whitelock and Buser [118] has η^L and η^U as given below:

$$\text{For cyclone No.1:} \quad 0.9 \ \leq \eta_1 \leq \ 0.99 \tag{3.43}$$

$$\text{For cyclone No.2:} \quad 0.55 \ \leq \eta_2 \leq \ 0.99 \tag{3.44}$$

$$\text{For cyclone No.3:} \quad 0.2 \ \leq \eta_3 \leq \ 0.99 \tag{3.45}$$

3.7   Results and discussion

All mathematical models have been implemented and solved in GAMS (General Algebraic Modeling System, [86]) in a CPU Intel Core i5-4200U, 1.60 GHz. CONOPT 3 solver [20] was used to solve the NLP problem.

The input feed as the parameters for both cyclone arrangements (parallel and series) to be processed is described in Table 3.1. The flow rate of input feed to the cyclones in both arrangements is roughly the sum of all particulates' flow rate that is generated from the two dryers, the cooler, and the screen of the proposed NPK plant. These data are used to calculate the optimal number of cyclones (N) of parallel arrangement while minimizing the total cost. In addition, to compute the value of optimal number of cyclones, the models

Parameter	Value
Q	13.97 (m^3/s)
ρ_p	1042.0 (kg/m^3)
ρ	1.33 (kg/m^3)
μ	19.34 x 10^{-6}($N.s/m^2$)
d$_p$	21.63 x 10^{-6}(m)

Table 3.1: Specification of input feed to the cyclone

calculate the optimal value of the pressure drop, the inlet velocity, and the diameter of the cyclone. The diameter of the cyclone has an important role in the resultant value of the pressure drop and the inlet velocity in this optimization. Therefore, after determination of the optimal number of cyclones with minimum cost, the optimal value of the diameter of the cyclone is obtained. Moreover, the value of the optimal diameter of the cyclone is used to calculate the optimal pressure drop and inlet velocity. Another value that affects the result of the optimization model is the value of efficiency of the cyclone, however this only applies for the series cyclone arrangement (Figure 3.3).

The obtained optimal number of cyclones lies within the constraints of the pressure drop of the cyclone, the inlet velocity, and the diameter of the cyclone. An interesting result arises in the optimization of which the optimal number of cyclones lies at the upper bound of the diameter. The selection of the upper bound of the diameter as the optimal value of the decision variable can be explained physically wherein by increasing the cyclone diameter, the residence time also increases. The increase in the available time for collection of particles results in an increase in the total collection efficiency. So, the optimal performance of the cyclone can be reached.

After the first trial, the constraint of the diameter as shown in Eq.(3.41) does not lead to draw a specific inference when it is used to find the optimal number of cyclones. This is probably due to a big gap between the lower bound and upper bound of the diameter. In order to obtain a specific result of the optimal number of cyclones, the constraint of

the diameter is modified. The constraints of the diameter of the cyclone are divided into five parameters (i.e., each parameter has a lower limit of 1.2 m and an upper limit varying between 1.8 m, 2.0 m, 2.5 m, 2.7 m, and 3.0 m). Moreover, these new constraints would be used to calculate the optimal number of the cyclone for each arrangement (i.e., parallel and series).

The resultant value of the optimization of the parallel 1D3D cyclone arrangement can be seen in Table 3.2. The optimal values of number of cyclones, the cyclone diameter, the cyclone pressure drop, and the inlet velocity of the cyclone of 1D3D cyclone were obtained by using the upper bound of diameter up to 2.5 m. Meanwhile, for the 2D2D cyclone (Table 3.3) and 1D2D cyclone (Table 3.4) the values of the optimal parameters are obtained using the upper bound of diameter up to 3.0 m and 2.7 m, respectively. The effects of the constraint of cyclone diameter on the results of optimal number of each type of cyclones connected in parallel are presented in Figure 3.5. The 1D3D cyclones connected in parallel have the smallest diameter for the same value of optimal number of cyclones (N = 3) compared with the other two. Using an upper bound diameter up to 3.0 m, the 2D2D cyclone with parallel arrangement model resulted in one cyclone as the optimal number of cyclones.

Furthermore, the simulation results obtained from the present mathematical programming models were also compared with the outputs of some other models, such as Yetilmezsoy's optimum body diameter (OBD) model [121, 122] and KalenZenz's model [58]. Detailed mathematical definitions of these models and relevant calculation procedures can be found in the studies of Yetilmezsoy [121, 122]. Based on the present input data (Q = 13.97 m^3/s, ρ_p = 1042kg/m^3, design temperature = 45 ^oC, a_0 = a/D = 0.50, and b_0 = b/D = 0.25), all models were evaluated for each type of cyclones (i.e., 1D3D, 2D2D, and 1D2D) connected in parallel, and the numerical outputs (i.e., cyclone diameter and pressure drop) were compared with the optimization results given in Tables 3.2 - 3.4. Table 3.5 lists comparisons of cyclone diameters and pressure drops predicted by the different models for 1D3D, 2D2D, and 1D2D cyclones at their own gas outlet diameter of the cyclone ratio ($De_0 = D_e/D$), i.e., 0.50, 0.50 and 0.625, respectively.

Parameter	1D3D Cyclone				
	Boundary of Diameter (m)				
	Low=1.2	Low=1.2	Low=1.2	Low=1.2	Low=1.2
	Up=1.8	Up=2.0	Up=2.5	Up=2.7	Up=3.0
Total cost ($/s)[a]	0.001	0.001	0.001	0.001	0.001
Number of cyclone	2.80	2.22	2.05	2.05	2.05
Diameter (m)	1.52	1.64	1.69	1.69	1.69
Pressure drop (N/m^2)	1223	1427	1505	1505	1505
Inlet velocity (m/s)	17.29	18.68	19.17	19.17	19.17

[a] 1 United States Dollar (USD, $) = 11,567.2 Indonesian Rupiah (IDR) (27-Apr-2014, 18:20 pm)

Table 3.2: Optimization results from GAMS code for 1D3D cyclones in parallel

Parameter	2D2D Cyclone				
	Boundary of diameter (m)				
	Low=1.2	Low=1.2	Low=1.2	Low=1.2	Low=1.2
	Up=1.8	Up=2.0	Up=2.5	Up=2.7	Up=3.0
Total cost ($/s)[a]	0.001000	0.001000	0.000947	0.000889	0.000869
Number of cyclone	2.46	1.98	1.25	1.06	1.00
Diameter (m)	1.80	2.00	2.50	2.70	2.78
Pressure drop (N/m^2)	807	819	844	852	854
Inlet velocity (m/s)	14.04	14.14	14.36	14.43	14.44

[a] 1 United States Dollar (USD, $) = 11,567.2 Indonesian Rupiah (IDR) (27-Apr-2014, 18:20 pm)

Table 3.3: Optimization results from GAMS code for 2D2D cyclones in parallel

	1D2D Cyclone				
	Boundary of diameter (m)				
Parameter	Low=1.2	Low=1.2	Low=1.2	Low=1.2	Low=1.2
	Up=1.8	Up=2.0	Up=2.5	Up=2.7	Up=3.0
Total cost ($/s)[a]	0.001000	0.001000	0.000888	0.000886	0.000886
Number of cyclone	2.456	1.998	1.360	1.350	1.350
Diameter (m)	1.8	1.99	2.26	2.26	2.26
Pressure drop (N/m^2)	589	597	771	774	774
Inlet velocity (m/s)	14.04	14.14	16.08	16.10	16.10

[a] 1 United States Dollar (USD, $) = 11,567.2 Indonesian Rupiah (IDR) (27-Apr-2014, 18:20 pm)

Table 3.4: Optimization results from GAMS code for 1D2D cyclones in parallel
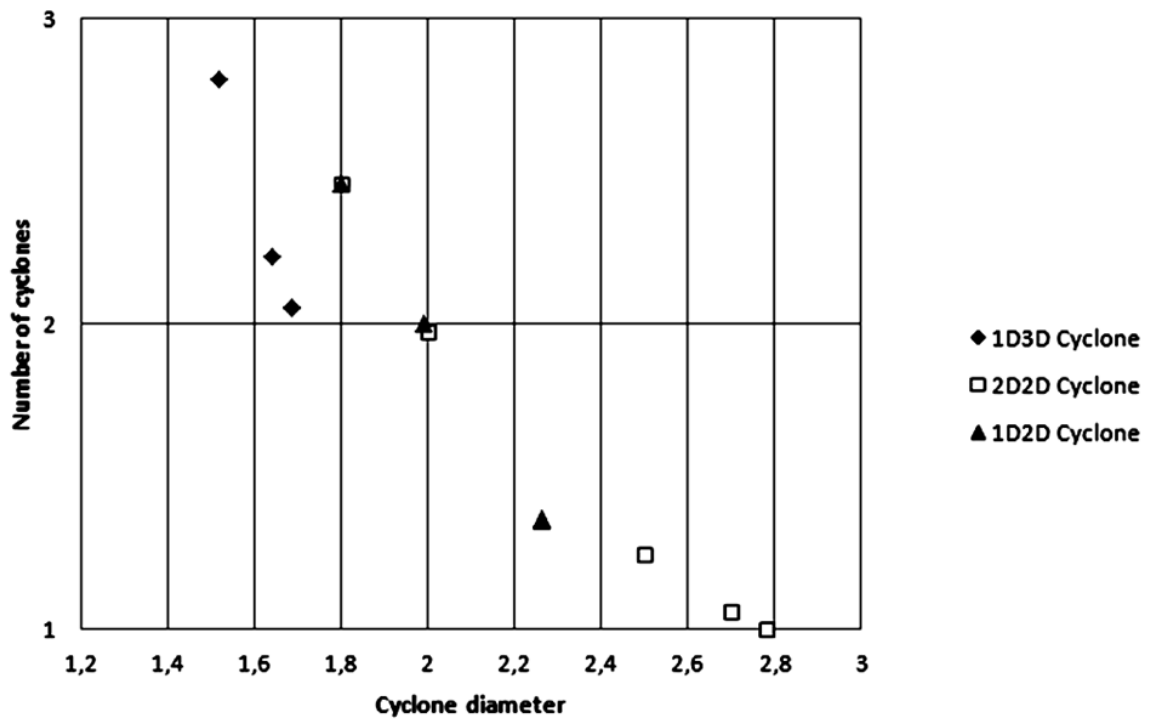
Figure 3.5: Optimal solution of parallel cyclone arrangement

Cyclone design	Number of cyclone	Present study		Yetilmezsoy's model		Kalen and Zenz's model	
		D_p (m)	ΔP_p (N/m^2)	D_p (m)	ΔP_p (N/m^2)	D_p (m)	ΔP_p (N/m^2)
1D3D ($De_0 = 0.50$)	2.80	1.52	1223	2.0333	893.19	1.6906	1868.9
	2.22	1.64	1427	2.2592	932.16	1.8785	1950.4
	2.05	1.69	1505	2.3425	945.93	1.9477	1979.2
	2.05	1.69	1505	2.3425	945.93	1.9477	1979.2
	2.05	1.69	1505	2.3425	945.93	1.9477	1979.2
2D2D ($De_0 = 0.50$)	2.46	1.80	807	2.1564	914.72	1.7929	1913.9
	1.98	2.00	819	2.3797	951.99	1.9786	1991.9
	1.25	2.50	844	2.9323	1036.1	2.4381	2167.8
	1.06	2.70	852	3.1602	1068.0	2.6276	2234.6
	1.00	2.78	854	3.245	1079.5	2.6981	2258.7
1D2D ($De_0 = 0.625$)	2.456	1.80	589	2.158	667.05	1.7943	1395.7
	1.998	1.99	597	2.3699	692.87	1.9705	1449.7
	1.360	2.26	771	2.8222	743.68	2.3465	1556.0
	1.350	2.26	774	2.8316	744.69	2.3544	1558.2
	1.350	2.26	774	2.8316	744.69	2.3544	1558.2

Table 3.5: Comparison of predicted cyclone diameters and pressure drops for 1D3D, 2D2D and 1D2D cyclones in parallel arrangement

The comparisons illustrated that the present study gave pressure drop predictions that were closest to the outputs obtained from the empirical methodology proposed by Yetilmez-soy [121, 122]. On the other hand, the numerical results in Table 3.5 confirmed that cyclone diameters obtained by the present study (GAMS code) were much closer to the theoretical outputs for 2D2D cyclone design than those calculated for 1D3D and 1D2D cyclones in parallel arrangement.

The cyclone configuration of series arrangement is influenced by the optimization of the efficiency of each cyclone. For example, the optimal configuration of two 1D3D cyclones in series will have 2.7 m of cyclone diameter with 97.8% of cyclone No.1 efficiency and 55% of cyclone No.2 efficiency (Table 3.6). Meanwhile for the three 1D3D cyclones in series, the efficiency of cyclone No.1 is found to be slightly lower (i.e., 97.2%) than the first cyclone in the two series cyclone arrangement. In addition, the efficiency of cyclone No.3 is only 20%. The other optimization results of 2D2D cyclone and 1D2D cyclone can be seen in Table 3.7 and Table 3.8, respectively. From these results, it can be concluded that in order to minimize the total cost and maximizing the overall efficiency, the optimal value of cyclone diameter lies at its upper bound. The selection of upper bound as the optimal value of the diameter of cyclone is in accordance with the results from Ravi et al. [83] method that selects the H_0 ratio (H/D) at its upper bound to increase the collection efficiency. In addition, in computing the optimal value of cyclone 2D2D diameter, the optimization using the series arrangement model gives the same result compared with the parallel arrangement model when using the upper bound of diameter at 3.0 m (Table 3.3). This shows that one 2D2D cyclone with a diameter of 2.7 m is appropriate to tackle the feed in this work with efficiency around 97%, then if it is added one more similar cyclone arranged in series, the overall efficiency can be increased up to 99%. Another result found from this study that by using the similar diameter as the first cyclone, the optimum efficiency of the secondary and tertiary cyclone lies at its lower bound. This result is found to be in line with the fact that since most of large particles are captured in the first cyclone, only small sized materials enter to the next stages. So with the optimum value of diameter lies at its upper bound, the model select the lower bound as its optimum value of the efficiency of cyclone

after stage one in order to minimize the total cost. A higher efficiency of the second or third stage cyclone can only be reached when using a smaller diameter or dimensions than the first cyclone.

Parameter	1D3D cyclone				
	2 cyclones in series		3 cyclones in series		
	Cycone No.1	Cyclone No.2	Cycone No.1	Cyclone No.2	Cyclone No.3
Efficiency (%)	97.8	55	97.2	55	20
Cut-size diameter (m)	30.77×10^{-6}	206.41×10^{-6}	30.77×10^{-6}	184.62×10^{-6}	275.21×10^{-6}
Diameter (m)	2.709	2.709	2.709	2.709	2.709
Pressure drop (N/m^2)	949.634	949.634	949.635	949.635	949.636
Inlet velocity (m/s)	15.232	15.232	15.232	15.232	15.232
Total cost (\$/s)[a]	0.002		0.003		
Overall efficiency (%)	99		99		

[a] 1 United States Dollar (USD, \$) = 11,459.3 Indonesian Rupiah (IDR) (14-May-2014, 21:22:28)

Table 3.6: Optimal solution of 1D3D cyclone series arrangement

Parameter	2D2D cyclone				
	2 cyclones in series		3 cyclones in series		
	Cycone No.1	Cyclone No.2	Cycone No.1	Cyclone No.2	Cyclone No.3
Efficiency (%)	97.8	55	97.2	55	20
Cut-size diameter (m)	19.86×10^{-6}	133.24×10^{-6}	19.86×10^{-6}	119.17×10^{-6}	177.65×10^{-6}
Diameter (m)	2.709	2.709	2.709	2.709	2.709
Pressure drop (N/m^2)	949.636	949.636	949.635	949.635	949.636
Inlet velocity (m/s)	15.232	15.232	15.232	15.232	15.232
Total cost (\$/s)[a]	0.002		0.003		
Overall efficiency (%)	99		99		

[a] 1 United States Dollar (USD, \$) = 11,459.3 Indonesian Rupiah (IDR) (14-May-2014, 21:22:28)

Table 3.7: Optimal solution of 2D2D cyclone series arrangement

Parameter	1D2D cyclone				
	2 cyclones in series		3 cyclones in series		
	Cycone No.1	Cyclone No.2	Cycone No.1	Cyclone No.2	Cyclone No.3
Efficiency (%)	97.8	55	97.2	55	20
Cut-size diameter (m)	22.207×10^{-6}	148.97×10^{-6}	22.21×10^{-6}	133.23×10^{-6}	198.61×10^{-6}
Diameter (m)	2.549	2.549	2.549	2.549	2.549
Pressure drop (N/m^2)	882.834	882.779	882.864	882.864	882.858
Inlet velocity (m/s)	17.2	17.201	17.201	17.201	17.201
Total cost ($/s)[a]	0.002		0.002		
Overall efficiency (%)	99		99		

[a] 1 United States Dollar (USD, $) = 11,459.3 Indonesian Rupiah (IDR) (14-May-2014, 21:22:28)

Table 3.8: Optimal solution of 1D2D cyclone series arrangement

The optimization results show that there is a significant difference of the pressure drop among all three types of cyclones (i.e., 1D3D, 2D2D, and 1D2D) where the 1D2D cyclone will have the lowest pressure drop with the smallest size of diameter (i.e., 2.5 m). In other words, the results of this study illustrate that the 1D2D cyclone in a series is more suitable to handle a given input feed. Additionally, two cyclones in series is more likely to be operated than three cyclones because as can be seen in the results, the total cost and total pressure drop in the system of three cyclones in series is higher than the two cyclones in series. The predictions of total pressure drop obtained by the model are found to be in accordance with the experimental measurements by Whitelock and Buser [118] which shows that the use of three cyclones in series increases the total pressure drop of the arrangement.

Based on the above-noted facts, the numerical findings also verified that pressure drops of cyclones could be accepted, since the values were obtained in the range of $500 \leq P \leq 2500$ N/m^2 [10]. The pressure drop values are found to be in line with the values reported by Wang et al. [112], who proposed a theoretical approach for predicting number of turns and cyclone pressure drop for 1D2D, 2D2D, and 1D3D cyclones at different inlet velocities of $v_{1D3D} = 16$ m/s, $v_{2D2D} = 15$ m/s, and $v_{1D2D} = 12$ m/s. Considering the nonlinear nature of the present problem, it should be noted that some differences may be expected

due to the applied mathematical techniques, different correlations, and different empirical coefficients used in the models proposed by various researchers. Since the solver status from CONOPT 3 is "*Optimal solution* [20]", it can be concluded that the capability of GAMS software in handling a nonlinearity from the proposed model is reliable.

3.8   Chapter Summary

In this chapter, mathematical programming models aimed at obtaining the best configuration of series and parallel cyclone arrangement in the NPK fertilizer plant are developed. A nonlinear programming model is considered in the present study where the optimal number and configuration of cyclones are optimized with respect to the minimum total cost including the operating cost and the capital cost. Different types of cyclones, in both arrangements, result in different optimal numbers of cyclones. Each type of cyclone (i.e., 1D3D, 2D2D, and 1D2D) has an alternative that can be arranged either in parallel or in series configuration, or even just a single cyclone. The cyclone diameter becomes a basic consideration because it determines the overall size of the cyclone, especially for the cyclone height. As a result of this study, if the available space is limited on the field, it is advised to choose the small cyclone with a small number of the cyclone arrangement. The last considerable value is the pressure drop of the cyclone. The pressure drop across the cyclone is directly related to the fan power requirement. Therefore, it is important to have the lowest pressure drop to have the lowest possible operating cost.

Chapter 4

Mixed Integer Nonlinear Programming Optimization of Multiple Cyclone Arrangement

The key idea of the present mathematical programming model is to present the capability of GAMS/DICOPT in solving the multiple cyclone arrangement problem. A MINLP model is considered in the present study to find the best cyclone arrangement with the optimal number of cyclones and dimensions from four combinations of 1D3D and 2D2D cyclones arranged in parallel-series with respect to the minimum total cost including the operating cost and the capital cost. The organization of this chapter is as follows: The basic idea and overview of the proposed model is presented in Section 4.1. Section 4.2 describes the problem statement and the input parameters for the optimization. A MINLP formulation along with the objective function of the optimization and all constraints are described in Section 4.3. Section 4.4 presents the three decision variables (N, D, and η_{ov}) that are involved in selecting the best cyclone arrangement from four levels (1D3D+1D3D, 2D2D+2D2D, 1D3D+2D2D, and 2D2D+1D3D). The sensitivities of optimal solution to various parameters are also discussed. A summary of this work is presented in Section 4.5.

4.1 Overview of proposed model

Cyclone separators have been used extensively during this century as a major gas-cleaning device and an effective technology for particulate matters (PM) control. Due to the wide range of industrial applications of the cyclone separator and the large number of different cyclone types and sizes available, a solution yielding the lowest total cost possible is naturally desired. Many studies have been conducted and reported based on experimental, theoretical, and computational research on the cyclones. The majority of these models have focused on the development of single cyclones. However, only a small number of researchers such as Gerrard and Liddle [38], Martinez-Benet and Casal [72], Ravi et al. [83], Swamee et al. [103], and Abdul-Wahab et al. [2] presented methods for obtaining the optimum values of the number of cyclones to be used in parallel. The use of multiple cyclones can be considered as one solution to the demands of obtaining the best pollution control strategies to achieve a minimum level of pollution reduction.

The growing developments on the general structural optimization problems (e.g., Grossman [44], [47], [48], [49]) have given the possibility to obtain new method to the solution of cyclone arrangement problems. The work that has been done in the optimization of pump configurations by Pettersson and Westerlund [77] and Westerlund et al. [117] has made it possible to obtain an effective formulation for the cyclone arrangement problem. Based on the results of those works and combined with the use of modern tools of optimization (i.e., GAMS [86]) to deliver the best results, a novel optimization of parallel-series cyclone arrangement will be presented in this study. A mixed integer nonlinear programming (MINLP) approach will be used to solve the problem. According to this approach, the problem is solved through the methodologies that successively solve mixed integer linear (MILP) approximations to the model, and NLP problems for fixed configurations [108].

The different types of cyclones that will be involved in the optimization are 1D3D [75] and 2D2D cyclones [95]. Wang et al. [115] reported that, compared to other cyclone designs, the 1D3D and 2D2D cyclones are the most efficient cyclone collectors for particle diameters less than 100 μm. Experimental studies using these cyclones in series have been

performed by some researchers to observe the effectiveness of these devices in capturing particulate matter. An existing 2D2D cyclone was connected to other 2D2D cyclone for the first test and to a 1D3D cyclone for the second test by Gillum et al. [40]. The results showed that the overall efficiency of 2D2D-1D3D in series (99.82 %) was higher than 2D2D-2D2D (99.78 %) where the pressure drop across the secondary 1D3D cyclone (1115 Pa) was higher than the 2D2D secondary cyclone (1010 Pa). Gillum and Hughs [39] found that the inlet velocity varied from 11.8 to 18.3 m/s through the two cyclones in series, 2D2D primary and 2D2D or 1D3D secondary, didn't affect the collection efficiency. Meanwhile, the total system pressure drop was drastically different for the lower inlet velocity (1207 Pa) compared to the higher inlet velocity (2852 Pa). Columbus [15] also studied a 2D2D primary cyclone in series with a 1D3D secondary cyclone in capturing particulate matters (PM) emitted from a seed cotton separator. The results showed that the overall efficiency of the arrangement was 97 % in the first study and 96.4 % in the second followed by a very high pressure drop in all treatments. Whitelock and Buser [118] evaluated the effectiveness of up to four 1D3D cyclones in series on heavy loading of particulate air streams (236 g/m^3). The study showed that the series arrangement had a significant improved in cyclone overall efficiency (97 %) compared to a single cyclone (91 %). However, having the two cyclones in series appeared to be the best choice because of the use of three or four 1D3D cyclones in series only slightly increased the overall efficiency along with a significant increase in the pressure drop across all cyclones.

All experimental studies exploring multi cyclones arrangements has given an idea to develop a mathematical model in order to solve a typical industrial emission problem. Therefore, the main objective of this study is to present a MINLP (Mixed Integer Nonlinear Programming) model to find the best cyclone arrangement with the optimal number of cyclones and dimensions from several combinations of 1D3D and 2D2D cyclones arranged in parallel-series for a high volume and heavy loading of solid particles. The objective function is to minimize the total cost, including the operating cost and the capital cost.

4.2   Problem Statement
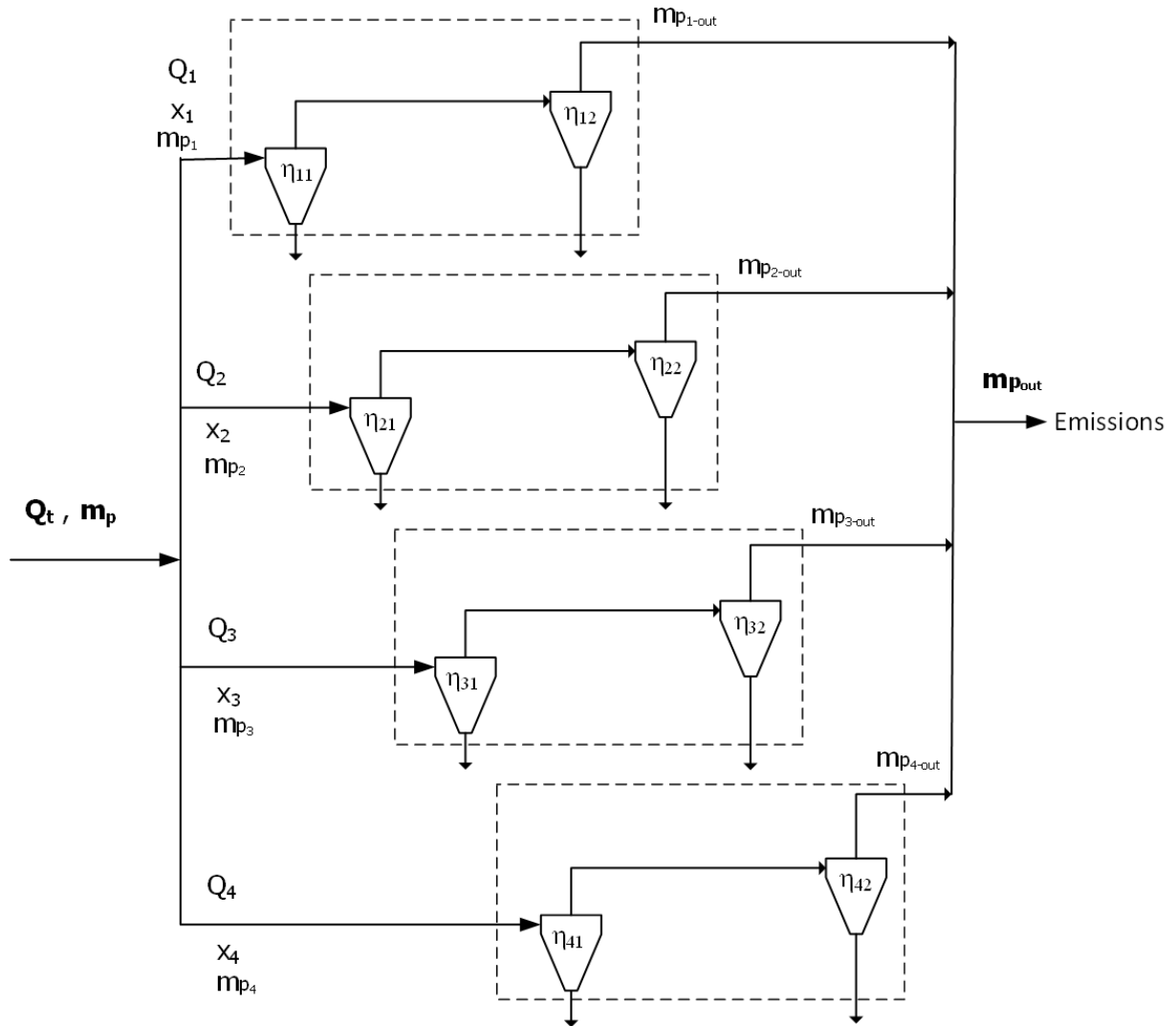
Figure 4.1: Four levels cyclone arrangement

The problem of multiple cyclone arrangement can be expressed as follows: for a given input feed, it is desired to determine the best cyclone arrangement of n parallel cyclone lines $(n = 1, 2, ..., N_p)$ with s $(s = 1, 2, ..., N_s)$ series cyclones in each line from various k

levels ($k = 1, 2, ..., N_K$) while minimizing the total cost. In addition, the efficiency of the cyclone system is expected to be maximized. Since these objectives are not conflicting with each other, i.e., the minimizing of the total cost will lead to maximize the efficiency of the cyclone, the model can obtain the optimal solution simultaneously. On each level a number of similar dimensions of cyclones are connected in parallel-series as can be seen in Figure 4.1. Furthermore, the cyclones in the parallel lines are actually the duplication units and the number of cyclone in series is considered as a stage of separation. In this way, there is an allowance for varying the number of stages to be considered for the separation task. However, the cyclone arrangement in this optimization is expected to have two (2) stages ($N_s = 2$). This upper bound is taken based on the feasible results from experiments conducted by Whitelock and Buser [118] which shows that the use of three or four identical cyclones in series increases the efficiency only slightly along with a significant increase in the pressure drop across all cyclones. The results from our previous study [2] also support that the two cyclones in series is more likely to be operated than three cyclones. In addition, there are four (4) levels that are considered in this optimization where the composition of each level is given in Table 4.1.

Level	Cyclone No.1	Cyclone No.2
1	1D3D	1D3D
2	2D2D	2D2D
3	1D3D	2D2D
4	2D2D	1D3D

Table 4.1: Composition of each level

The configuration / dimensions ratios of cyclones 1D3D and 2D2D can be seen in Table 4.2. The input feed data provided by Ravi et al. [83] is used in this study and as shown in Table 4.3. A total flow rate (Q) of 165 m^3/s represents a stream to be processed in a paper mill [7, 83].

Ratio	Cyclone 1D3D	Cyclone 2D2D	Cyclone 1D2D
$a_0 = \frac{a}{D}$	0.5	0.5	0.5
$b_0 = \frac{b}{D}$	0.25	0.25	0.25
$S_0 = \frac{S}{D}$	0.125	0.125	0.625
$D_{e_0} = \frac{D_e}{D}$	0.5	0.5	0.625
$H_0 = \frac{H}{D}$	4	4	3
$h_0 = \frac{h}{D}$	1	2	1
$B_0 = \frac{B}{D}$	0.25	0.25	0.5

Table 4.2: Cyclone configuration ratio

Parameter	Value
Q	165 (m^3/s)
ρ_p	1600 $(\mathrm{kg/m}^3)$
ρ	0.7895 $(\mathrm{kg/m}^3)$
μ	24.8 x $10^{-6}(N.s/m^2)$
MMD	10 x $10^{-6}(m)$
GSD	2.5

Table 4.3: Specification of input feed to the cyclone system

4.3 MINLP formulation

4.3.1 Objective function

The total flow rate through the arrangement, Q_t, is the summation of the flow rate of each level k, Q_k, as expressed in Eq.(4.1).

$$Q_t = \sum_{k=1}^{N_K} Q_k \qquad (4.1)$$

$$N_K \triangleq \text{ number of level of the cyclone arrangement}$$

Where the distribution of the flow rate through each level k is calculated using Eq.(4.2).

$$Q_k = Q_t \; x_k \qquad (4.2)$$

where:

$$\sum_{k=1}^{N_K} x_k = 1 \qquad (4.3)$$

$$x_k \triangleq \text{ the fraction of total flow through level k}$$

For all cyclones on each parallel line through all the stages, the input flow rate, Q_p, is the same and prorated over the number of parallel lines (N_p).

$$Q_{p_k} = \frac{Q_k}{N_{p_k}} \qquad (4.4)$$

where:

$$N_{p_k} \triangleq \text{ the number of parallel lines on level k}$$

It is assumed that the mass fraction has the same value with the volume fraction. So that, the mass of particle that goes through the first cyclone of each level can be calculated by using Eq.(4.5).

$$m_{p1k} = m_p\, x_k \tag{4.5}$$

Meanwhile, since the input feed for the second cyclone is actually the overflow from the first cyclone, the mass of particle that goes to the second cyclone will be affected by the efficiency of cyclone number one.

$$m_{p2k} = (1 - \eta_{1k})\, m_{p1k} = (1 - \eta_{1k})\, m_p\, x_k \tag{4.6}$$

where:

$$\eta_{1k} \triangleq \text{the efficiency of the first cyclone on level k}$$

Furthermore, the illustration given in Figure 4.2 is used to calculate the overall efficiency of the arrangement. There are two types of mass balance involved in calculating the mass of the emission of the cyclone system ($m_{p_{out}}$): First, it can be calculated by summing each mass of particle emitted from the last stage as stated in Eq.(4.7). Second, it can be calculated by assuming that the cyclone system as the one big cyclone and it has an overall cyclone (η_{ov_t}), yields Eq.(4.8).
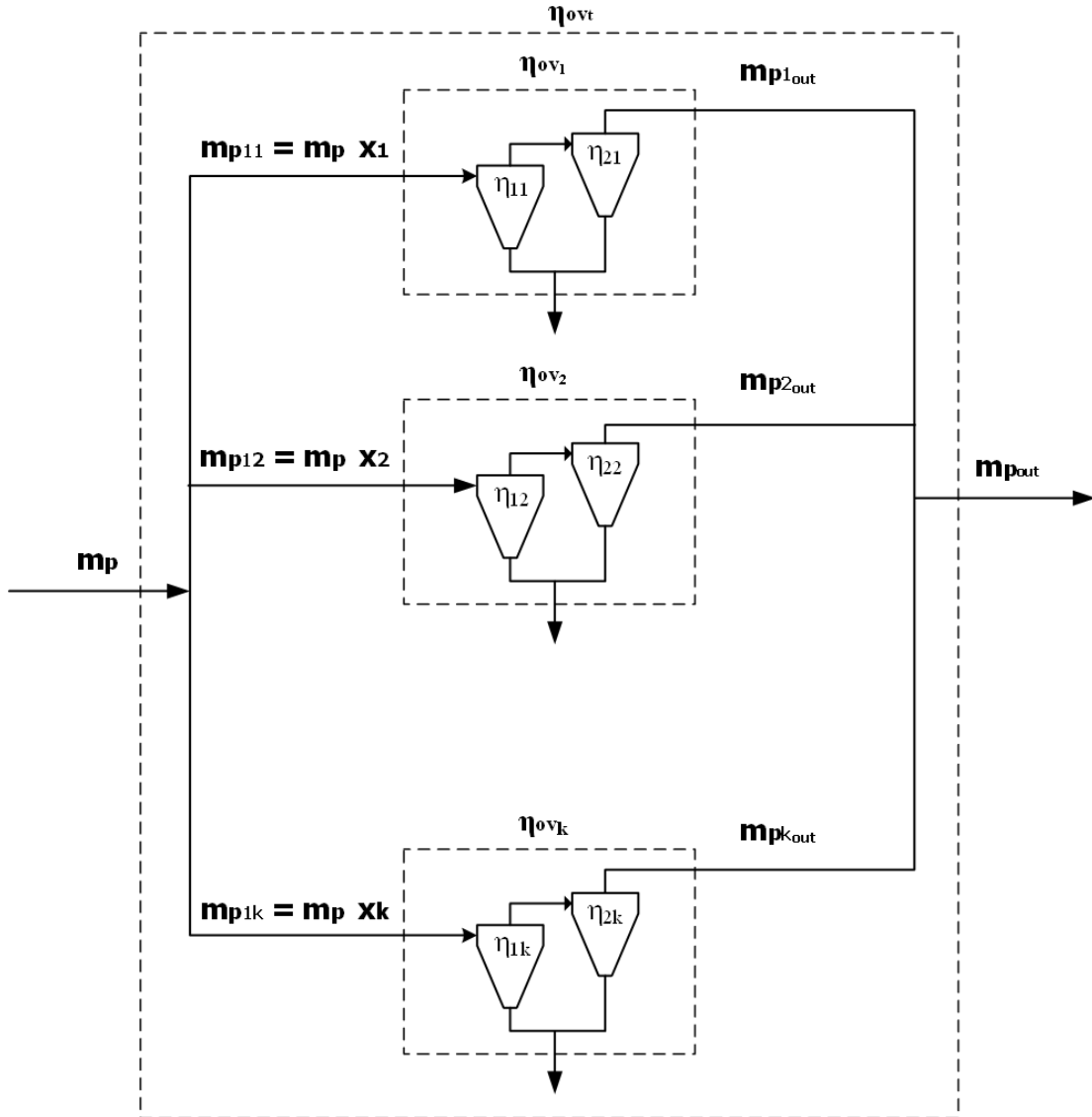
Figure 4.2: Illustration of the overall efficiency of the cyclone system

$$m_{p_{out}} = \sum_{k=1}^{N_K} m_{p_{k out}} = \sum_{k=1}^{N_K}(1 - \eta_{ov_k})\, m_{p_{1k}} = \sum_{k=1}^{N_K}(1 - \eta_{ov_k})\, m_p\, x_k \qquad (4.7)$$

$$m_{p_{out}} = (1 - \eta_{ov_t})\, m_p \qquad (4.8)$$

Combining Eqs.(4.7) - 4.8) gives Eq.(4.9).

$$\eta_{ov_t} = 1 - \left[\sum_{k=1}^{N_K} \{ (1 - \eta_{ov_k}) \, x_k \} \right] \tag{4.9}$$

where:

$$\eta_{ov_k} = 1 - [(1 - \eta_{1k})(1 - \eta_{2k})] \tag{4.10}$$

$\eta_{ov_k} \triangleq$ the overall efficiency of the parallel-series cyclone arrangement on level k

$\eta_{ov_t} \triangleq$ the overall efficiency of the cyclone system

In order to calculate the collection efficiency of individual cyclones, there are several theoretical models available in the literature. In this study, the observation reported by Wang et al. [111, 113, 114, 115] who established that the efficiency of cyclone systems is a function of the particle size distribution (PSD) will be used to calculate the theoretical model of cyclone overall efficiency. If it is assumed that the inlet particle size distribution is a lognormal distribution with mass median diameter (MMD) and geometric standard deviation (GSD), then the log-normal distribution function can be used to calculate the particle collection probability as shown in Eq.(4.11) [23] [68].

$$F(d_p) = \int_{d_p}^{\infty} \frac{1}{\sqrt{2\pi} \, d_p \, ln(GSD)} \, exp \left[-\frac{1}{2} \left(\frac{ln(d_p) - ln(MMD)}{ln(GSD)} \right)^2 \right] dd_p \tag{4.11}$$

According to Wang et al. [111], if the value of the cut-size diameter is substituted into Eq.(4.11), the equation can be used to calculate the theoretical model of cyclone overall efficiency. However, it should be noted that the equation of the cut-size diameter shall be corrected by introducing a cut-size diameter correction factor (i.e., K_{1D3D} for cyclone 1D3D and K_{2D2D} for cyclone 2D2D.

$$K_{(1D3D)} = 5.3 \, + \, 0.02 \, MMD - 2.4 \, GSD \tag{4.12}$$

$$K_{(2D2D)} = 5.5 \, + \, 0.02 \, MMD - 2.5 \, GSD \tag{4.13}$$

The cut-size diameter correction factor provided by Wang et al. [111] will be used in this study. Thus, by putting the correction factor into the cut-size diameter equation shown in Eq.(4.14), the corrected cyclone cut-size diameter equation for cyclone 1D3D and cyclone 2D2D becomes as given in Eq.(4.15) and Eq.(4.16), respectively.

$$d_p = \left[\frac{9 \, \mu \, b}{\pi \, N_i \, (\rho_p - \rho) \, v_i} \right]^{\frac{1}{2}} \tag{4.14}$$

$$d_{p_{(1D3D)}} = K_{(1D3D)} \left[\frac{9 \, \mu \, b_{(1D3D)}}{\pi \, N_{i_{(1D3D)}} \, (\rho_p - \rho) \, v_i} \right]^{\frac{1}{2}} \tag{4.15}$$

$$d_{p_{(2D2D)}} = K_{(2D2D)} \left[\frac{9 \, \mu \, b_{(2D2D)}}{\pi \, N_{i_{(2D2D)}} \, (\rho_p - \rho) \, v_i} \right]^{\frac{1}{2}} \tag{4.16}$$

Eqs.(4.15) - 4.16) can be rearranged to observe a relationship between the mass of particle and cut-size diameter. The results are shown in Eq.(4.17) and Eq.(4.18).

$$d_{p_{(1D3D)}} = \frac{1}{K_{(1D3D)}^2} \frac{2 \, m_p \, N_{i_{(1D3D)}} \, v_i}{3 \, \mu \, b_{(1D3D)}} \tag{4.17}$$

$$d_{p_{(2D2D)}} = \frac{1}{K_{(2D2D)}^2} \frac{2 \, m_p \, N_{i_{(2D2D)}} \, v_i}{3 \, \mu \, b_{(2D2D)}} \tag{4.18}$$

In addition, since the efficiency of the first cyclone will affect the mass of particle that enter the second cyclone on each level, Eqs.(4.17) - 4.18) are altered into the following equations:

$$\text{As the first cyclone:} \quad d_{p_{(1D3D)_1}} = \frac{1}{K_{(1D3D)_1}^2} \frac{2 \, m_p \, x_k \, N_{i_{(1D3D)}} \, v_i}{3 \, \mu \, b_{(1D3D)}} \tag{4.19}$$

$$d_{p_{(2D2D)_1}} = \frac{1}{K_{(2D2D)_1}^2} \frac{2 \, m_p \, x_k \, N_{i_{(2D2D)}} \, v_i}{3 \, \mu \, b_{(2D2D)}} \tag{4.20}$$

$$\text{As the second cyclone:} \quad d_{p_{(1D3D)_2}} = \frac{1}{K_{(1D3D)_2}^2} \frac{2 \, (1 - \eta_{1k}) \, m_p \, x_k \, N_{i_{(1D3D)}} \, v_i}{3 \, \mu \, b_{(1D3D)}} \tag{4.21}$$

$$d_{p_{(2D2D)_2}} = \frac{1}{K_{(2D2D)_2}^2} \frac{2 \, (1 - \eta_{1k}) \, m_p \, x_k \, N_{i_{(2D2D)}} \, v_i}{3 \, \mu \, b_{(2D2D)}} \tag{4.22}$$

The equations for the inlet velocity of gas through level k, v_{i_k}, and the pressure drop of each cyclone on level k, ΔP_k, are the same form as indicated in Eq.(3.18) and Eq.(3.19), respectively. For present case, these equations can be rewritten as shown in Eq.(4.23) and Eq.(4.24).

$$v_{i_k} = \frac{Q_k}{N_{p_k} \, a_k \, b_k} = \frac{Q_k}{N_{p_k} \, a_{0_k} \, b_{0_k} \, D_k^2} \tag{4.23}$$

$$\Delta P_k = \frac{1}{2}\rho v_{i_k}^2 N_H = \frac{1}{2}\rho \left(\frac{Q_k}{a_{0_k} \, b_{0_k} \, D_k^2 \, N_{p_k}} \right)^2 N_H \tag{4.24}$$

The optimum configuration of the cyclone is highly dependent on the way to find the optimum diameter of the cyclone. The results from our previous study [2] has shown that the diameter of the cyclone has an important role in the resultant value of the pressure drop and the inlet velocity in the optimization. These aspects directly affect the total cost. In the present study, although the dimensions of the second cyclone are expected to be the same as the first cyclone, the equations that need to be used for the calculations are different.

If the cyclone 1D3D or 2D2D is arranged as the first cyclone, the diameter is calculated by rearranging and substituting Eq.(4.25) (the mass of the particle defined by Clift et al. [14]) and Eq.(4.23) into Eqs.(4.19) - 4.20), to yield Eqs.(4.26 - 4.27).

$$m_p = \left(\frac{\pi d_p^3}{6} \right) (\rho_p - \rho) \tag{4.25}$$

$$D_{(1D3D)_1} = \left[\frac{d_{p(1D3D)_1}^2 \, \pi \, N_{i(1D3D)} \, (\rho_p - \rho) \, x_k \, Q_k}{9 \, K_{(1D3D)_1}^2 \, \mu \, b_{1D3D_0}^2 \, a_{1D3D_0} \, N_{p_k}} \right]^{1/3} \tag{4.26}$$

$$D_{(2D2D)_1} = \left[\frac{d_{p(2D2D)_1}^2 \, \pi \, N_{i(2D2D)} \, (\rho_p - \rho) \, x_k \, Q_k}{9 \, K_{(2D2D)_1}^2 \, \mu \, b_{2D2D_0}^2 \, a_{2D2D_0} \, N_{p_k}} \right]^{1/3} \tag{4.27}$$

The equation that need to be used to calculate the diameter of cyclone when it is arranged as the second cyclone is obtained by rearranging and substituting Eq.(3.4) and

Eq.(4.23) into Eqs.(4.21) - 4.22), which yields Eqs.(4.28 - 4.29).

$$D_{(1D3D)_2} = \left[\frac{d^2_{p_{(1D3D)_2}} \pi N_{i_{(1D3D)}} (\rho_p - \rho) (1 - \eta_{1k}) x_k Q_k}{9 K^2_{(1D3D)_2} \mu b^2_{1D3D_0} a_{1D3D_0} N_{p_k}} \right]^{1/3} \qquad (4.28)$$

$$D_{(2D2D)_2} = \left[\frac{d^2_{p_{(2D2D)_2}} \pi N_{i_{(2D2D)}} (\rho_p - \rho) (1 - \eta_{1k}) x_k Q_k}{9 K^2_{(2D2D)_2} \mu b^2_{2D2D_0} a_{2D2D_0} N_{p_k}} \right]^{1/3} \qquad (4.29)$$

The purpose of the optimization is to find the best cyclone arrangement with the optimal number of cyclones and configuration / dimensions. The objective function is the total cost (c_{tot}) minimization, including the operating costs and the capital costs. The operating costs are considered as the overall operating costs of the arrangement of the cyclone, while the cost of capital is the total capital cost of each cyclone in parallel lines and at all stages. The equations to calculate the operating cost and the capital cost of the cyclone has been presented in Abdul-Wahab et al. [2]. Therefore the derivation of those equations will not be presented here, only the resulting formulations are shown here. The objective function of the optimization can now be expressed as indicated in Eq.(4.30):

$$MIN \ c_{tot} = \sum_{k=1}^{N_K} \left[Q_k \, c_e \, (\Delta P_{k_1} + \Delta P_{k_2}) \ + \ \frac{F \, e \, N_{p_k}}{Y \, t_w} \left(D^j_{k_1} + D^j_{k_2} \right) \right] \qquad (4.30)$$

where:

$c_{tot} \triangleq$ the total cost ($ / second)

$c_e \triangleq$ the cost of utilities (= $ 1.5 x $10^{-8}/J$ [97])

$F \triangleq$ investment factor (= 4.4 [99])

$Y \triangleq$ number of years over which depreciation occurs (= 5)

$t_w \triangleq$ time worked per year (= 2.16 x $10^7 s/year$)

$e \triangleq$ constant (= $ 4924.61/m) that is obtained from Eq.(3.16)

$j \triangleq$ constant (= 1.2) that its value depends on the equipment type [99]

4.3.2 Constraints

It is necessary to introduce binary (0-1) variables z for each level, defining the existence or nonexistence of the level. Therefore, a binary variable z_k defines the existence of any level if the flow rate through the level k has a nonzero value. The model is intended to find the best cyclone arrangement for handling a given feed, so the inequality of the binary variable is expressed as follows:

$$\sum_{k=1}^{N_K} z_k \leq 1 \tag{4.31}$$

The upper limit of the total flow rate and the parallel flow rate through level k is expressed as indicated in Eq.(4.32) and Eq.(4.33), respectively.

$$Q_k \leq Q_k^U \, z_k \tag{4.32}$$

$$Q_{p_k} \, N_{p_k} \leq Q_{p_k}^U \, z_k \tag{4.33}$$

The binary variables indicate the different intervals which are included in the formulation and thereby define the volume fractions, x_k, at the optimal solution. In order to ensure that there is always at least one existing level of the cyclone arrangement and to prevent the violation of the value of x_k over z_k. Hence, one more constraint will be added as shown as follows:

$$x_k - z_k \leq 0 \tag{4.34}$$

N_{p_k} is an integer variable, while Q_k, Q_{p_k}, and x_k are non-negative real variables. The number of cyclones as a decision variable must be restricted by the upper limit, $N_{p_k}^U$, of the number of parallel lines and should further be specified whether the level exists or not. The inequality can be written as follows:

$$N_{p_k} - N_{p_k}^U \, z_k \leq 0 \tag{4.35}$$

Two other decision variables besides N_{p_k} in this optimization are the diameter of the cyclone and the efficiency of the cyclone. The diameter of the cyclone is one of the most important aspects to find the optimum number of cyclones. According to Ravi et al. [83], a small diameter ranged from 0.3 to 0.7 m could be taken, while based on our previous study [2], the upper limit on diameter (D_k^U), is somewhat arbitrarily selected, at least to some extent, if the optimal solution lies at the upper bound. In addition, it is desired to have a maximum value of the efficiency while the total cost is minimized.

As mentioned earlier, by substituting the cut-size diameter into Eq.(4.11), the equation can be used to calculate the cyclone overall efficiency. Eq.(4.11) will be substituted by a surrogate model by finding a relationship between the cut-size diameter and the cyclone overall efficiency. Furthermore, by using PSD data in Table 4.3 (i.e., $MMD_1 = 10$ x 10^{-6} m and $GSD_1 = 2.5$) as an input, Figure 4.3 is produced and a global surrogate consisting of a polynomial of degree four will be used to find the optimal efficiency of the first cyclone. For the second cyclone, it is necessary to know the PSD of the particles that are emitted from the first cyclone. In this study, it is assumed that the ratio of overflow PSD and input feed PSD of the first cyclone obtained from experimental results of Whitelock and Buser [118] will be used, where the value of MMD_2 becomes 3.7 x 10^{-6} m and GSD_2 is assumed to have the same value (i.e., 2.5). Similarly, Figure 4.4 is used to find the optimal efficiency of the second cyclone.
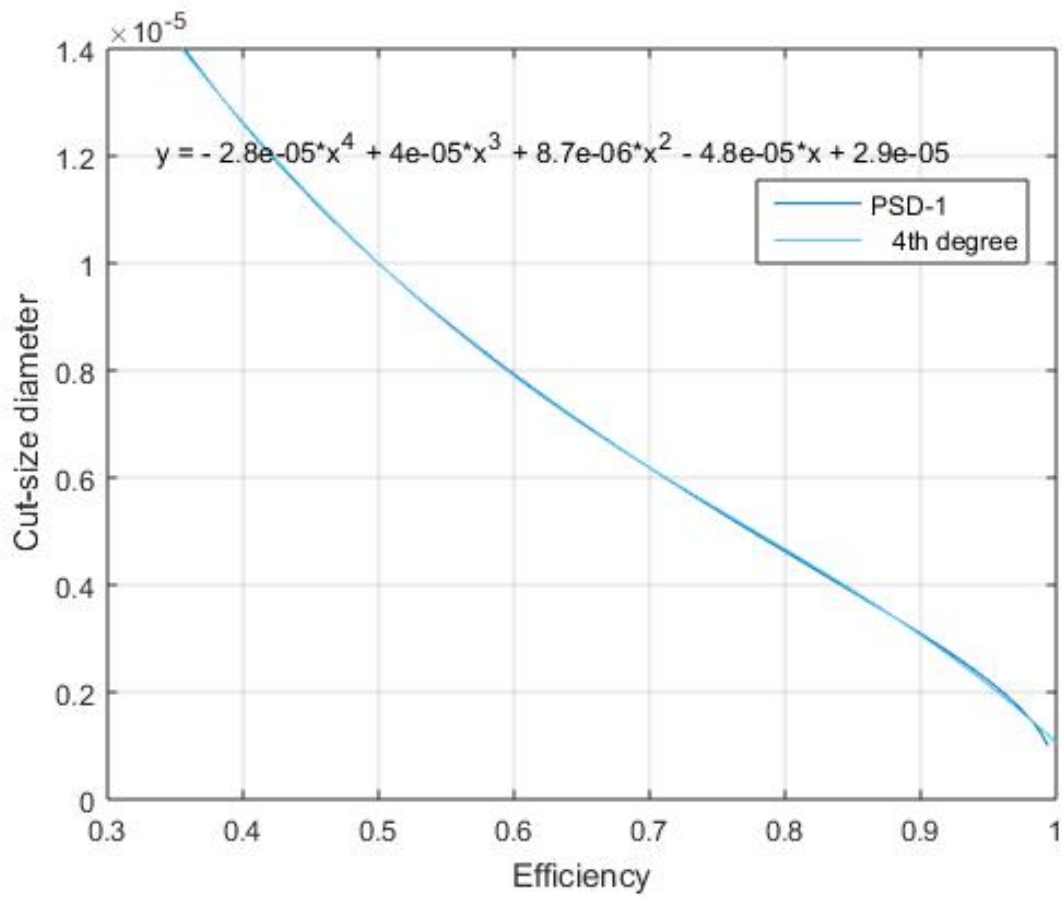
Figure 4.3: The efficiency vs the cut-size diameter for the first cyclone

The figure shows a plot with the equation:

$$y = 2.6e\text{-}05 \cdot x^4 - 8.3e\text{-}05 \cdot x^3 + 9.7e\text{-}05 \cdot x^2 - 5.5e\text{-}05 \cdot x + 1.6e\text{-}05$$

Axes: Cut-size diameter (y-axis, $\times 10^{-5}$) vs Efficiency (x-axis). Legend: PSD-2, 4th degree.
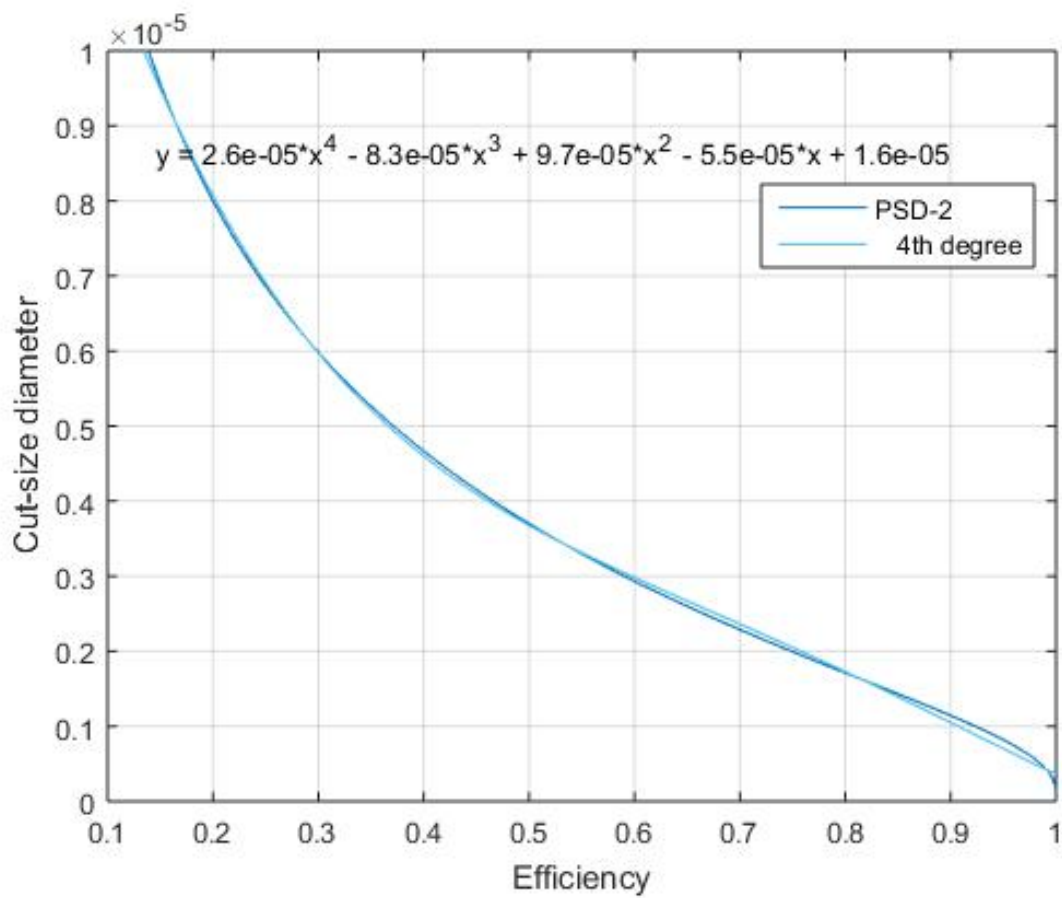
Figure 4.4: The efficiency vs the cut-size diameter for the second cyclone

The pressure drop and inlet velocity through the cyclone are the most important constraints in order to seek the optimum cyclone configuration with the lowest total cost. The upper bound of the pressure drop for each cyclone is generally expected not to exceed 2500 N/m^2 [72].

$$\Delta P_k^U \leq 2500 \ \ N/m^2 \tag{4.36}$$

The inlet velocity for identical size and configuration of cyclone has the relationship with the efficiency, where the higher the gas inlet velocity is, the higher the efficiency would be [41]. The constraint on the inlet velocity that is normally used in industrial practice lies in the range as shown in Eq.(4.37) [94].

$$15 \leq \ v_{i_k} \ \leq 30 \ \ m/s \tag{4.37}$$

The lower bound of inlet velocity $(v_{i_k}^L)$ is provided to ensure the values on efficiency of the cyclone are reasonably high, while the upper bound $(v_{i_k}^U)$ helps reduce excessively high values of ΔP_k, and re-entrainment of solids [83].

In addition, in order to ensure that the value of the diameter of the cyclone and the inlet velocity are equal to zero in the case when level k is not selected, the following constraints will be added to the model:

$$D_k^U - 3 \ z_k \ \leq \ 0 \tag{4.38}$$

$$v_{i_k}^U - 30 \ z_k \ \leq \ 0 \tag{4.39}$$

4.4   Results and discussion

All mathematical models were implemented in GAMS [86]. GAMS is a general modeling system which is designed to make the solution of complex optimization problems more straightforward. The MINLP problem in this study was solved using DICOPT (DIscrete

and Continuous OPTimizer) [25] that runs under GAMS. The MINLP algorithm inside DICOPT solves a series of MILP and NLP sub-problems where the MILP and NLP were solved using CPLEX [1] and CONOPT 3 [20], respectively. The program was run on a CPU Intel Core i5-4200U, 1.60 GHz CPU and 8 Gbyte memory. The algorithm in DICOPT is based on three key ideas: Outer Approximation (OA), Equality Relaxation (ER), and Augmented Penalty (AP). The program starts by solving the NLP in which the 0-1 conditions on the binary variables are relaxed. The search is terminated if the solution to the problem yields an integer solution. Otherwise, it continues with an alternating sequence of nonlinear programs (NLP) called subproblems and mixed-integer linear programs (MILP) called master problems. The NLP subproblems are solved for fixed 0-1 variables that are predicted by the MILP master problem at each (major) iteration. It should be noted that the NLP solution for the first step is only guaranteed to correspond to a global optimum if appropriate convexity conditions are satisfied. If the relaxed NLP has multiple local solutions, the algorithm is not guaranteed to reach the global optimum. Nonetheless, the numerical performance which has been tested on a variety of applications, has shown a high degree of reliability for finding the global optimum in nonconvex problems [108]. Details about the DICOPT algorithm and references to earlier work can be found in Viswanathan and Grossmann [108], Kocis and Grossmann [62], and Duran and Grossmann [22].

As the DICOPT will start solving the relaxed NLP subproblem, the constraints for the model must be selected appropriately so that all functions can be properly evaluated. In this optimization, the summary of the lower (a_i^L) and upper (a_i^U) bounds of the decision variables, a_i, are given in Table 4.4. As can been seen from Table 4.4, there are three decision variables used in the optimization. The earlier study by Bhaskar et al. [8] observed that by using two or more decision variables, the optimization problem tended to have very high degree of freedom. Therefore, referring to Ravi et al. [83], in order to minimize the degree of freedom in the present optimization, two decision variables (N and D or η_{ov} and D) are used to check the sensitivity of the model to the optimal solution.

i	a_i	a_i^L	a_i^U
1	N	1	500
2	D, m	0.3	3
3	η_{ov}, %	0	100

Table 4.4: Bounds on decision variables, a_i

The stopping criterion for finding the optimal solution in this optimization is based on the heuristic: stop as soon as the NLP subproblems stops improving (i.e., the current NLP subproblem has an optimal objective function that is worse than the previous NLP subproblem). This stopping criterion tends to work very well for a non-convex problem [25, 108]. In order to provide a better bound to help the optimization in finding the optimal solution and attaining the convergence, a reasonably wide range value of the decision variable N should be selected properly for each upper bound of the cyclone diameter, D. Moreover, the selection of these values can be determined in a priori manner.

Tables 4.5 - 4.14 present the optimization results for different upper bounds of cyclone diameter D_p^U and number of parallel lines N_p^U. As can be seen from the results, the optimal value of the cyclone diameter (D_p) lies at its upper bound (D_p^U). In this case the value of D_p^U is found to be the most important decision variable that will lead the model to obtain the optimal solution to the problem. The optimal value of the cyclone pressure drop remains constant for some range of D_p (i.e., $D_p = 0.3$ m - 0.8 m) since the optimal value of the inlet velocity lies in its upper bound. Thereafter, the trend of cyclone pressure drop will follow a decreasing trend of the inlet velocity as the number of parallel lines (number of cyclones) decreases. The search is stopped purposely at the value of 2.5 m of the upper bound of D_p since the resultant value of the overall efficiency (η_{ov_t}) becomes less than 30 % which is an unacceptable value in the industry.

D_p^U	N_p^U	k	D_p	N_p	η_1	η_2	η_{ov_t}	v_{i_p}	Δp	c_{tot}
0.3	500	3	0.3	489	0.835	0.201	0.868	30	2186.718	0.057

Table 4.5: Optimization result for $D_p^U = 0.3$ m and $N_p^U = 500$

D_p^U	N_p^U	k	D_p	N_p	η_1	η_2	η_{ov_t}	v_{i_p}	Δp	c_{tot}
0.4	300	3	0.4	275	0.786	0.197	0.828	30	2186.718	0.048
0.5	300	1	0.5	176	0.742	0.102	0.769	30	2186.718	0.042
0.6	300	1	0.6	123	0.704	0.0907	0.733	30	2186.718	0.037
0.8	300	3	0.8	70	0.639	0.173	0.701	30	2186.718	0.032
2.3	300	2	2.3	10	0.544	0.065	0.573	26.774	1741.711	0.019

Table 4.6: Optimization result for $D_p^U = 0.4$ - 0.6, 0.8, 2.3 m and $N_p^U = 300$

D_p^U	N_p^U	k	D_p	N_p	η_1	η_2	η_{ov_t}	v_{i_p}	Δp	c_{tot}
0.7	100	1	0.7	90	0.670	0.092	0.701	30	2186.718	0.034

Table 4.7: Optimization result for $D_p^U = 0.7$ m and $N_p^U = 100$

D_p^U	N_p^U	k	D_p	N_p	η_1	η_2	η_{ov_t}	v_{i_p}	Δp	c_{tot}
0.8	200	2	0.8	70	0.792	0.107	0.814	29.747	2150.056	0.032
1.0	200	2	1.0	47	0.737	0.101	0.764	28.029	1908.814	0.028
1.1	200	2	1.1	40	0.712	0.098	0.740	27.326	1814.208	0.027
1.3	200	2	1.3	30	0.666	0.091	0.696	26.135	1659.53	0.025

Table 4.8: Optimization result for $D_p^U = 0.8$, 1.0 - 1.1, 1.3 m and $N_p^U = 200$

D_p^U	N_p^U	k	D_p	N_p	η_1	η_2	η_{ov_t}	v_{i_p}	Δp	c_{tot}
0.9	400	2	0.9	57	0.764	0.104	0.789	28.828	2019.143	0.030

Table 4.9: Optimization result for $D_p^U = 0.9$ m and $N_p^U = 400$

D_p^U	N_p^U	k	D_p	N_p	η_1	η_2	η_{ov_t}	v_{i_p}	Δp	c_{tot}
1.2	250	2	1.2	35	0.688	0.095	0.718	26.699	1731.941	0.026
1.5	250	3	1.5	24	0.46	0.125	0.528	25.156	1537.615	0.023
1.6	250	2	1.6	21	0.607	0.08	0.639	24.727	1485.59	0.022
1.8	250	2	1.8	17	0.574	0.072	0.605	23.963	1395.14	0.021
2.1	250	2	2.1	13	0.544	0.065	0.573	24.446	1451.975	0.019
2.2	250	2	2.2	11	0.544	0.065	0.573	26.610	1593.551	0.019

Table 4.10: Optimization result for $D_p^U = 1.2, 1.5, 1.6, 1.8, 2.1, 2.2$ m and $N_p^U = 250$

D_p^U	N_p^U	k	D_p	N_p	η_1	η_2	η_{ov_t}	v_{i_p}	Δp	c_{tot}
1.9	350	2	1.9	16	0.558	0.069	0.589	23.620	1355.484	0.020
2.0	350	2	2.0	15	0.544	0.065	0.573	23.299	1318.899	0.020
2.4	350	3	2.4	9	0.368	0.096	0.428	26.656	1726.353	0.018

Table 4.11: Optimization result for $D_p^U = 1.9, 2.0, 2.4$ m and $N_p^U = 350$

D_p^U	N_p^U	k	D_p	N_p	η_1	η_2	η_{ov_t}	v_{i_p}	Δp	c_{tot}
1.7	450	2	1.7	19	0.59	0.076	0.621	24.331	1438.326	0.021

Table 4.12: Optimization result for $D_p^U = 1.7$ m and $N_p^U = 450$

D_p^U	N_p^U	k	D_p	N_p	η_1	η_2	η_{ov_t}	v_{i_p}	Δp	c_{tot}
1.3	30	2	1.3	30	0.666	0.091	0.696	26.135	1659.53	0.025
1.4	30	2	1.4	27	0.645	0.087	0.676	25.624	1595.248	0.024
1.5	30	2	1.5	24	0.626	0.083	0.657	25.156	1537.615	0.023
1.6	30	2	1.6	21	0.607	0.08	0.639	24.727	1485.59	0.022
1.7	30	2	1.7	19	0.59	0.076	0.621	24.331	1438.326	0.021
1.8	30	2	1.8	17	0.574	0.072	0.605	23.963	1395.14	0.021
1.9	30	2	1.9	16	0.558	0.069	0.589	23.620	1355.484	0.020
2.0	30	2	2.0	15	0.544	0.065	0.573	23.299	1318.899	0.020
2.2	30	2	2.2	11	0.544	0.065	0.573	26.610	1593.551	0.019
2.3	30	2	2.3	10	0.544	0.065	0.573	26.774	1741.711	0.019
2.4	30	2	2.4	9	0.544	0.065	0.573	27.192	1796.529	0.019
2.5	30	2	2.5	10	0.486	0.050	0.512	22.516	1231.795	0.017

Table 4.13: Optimization result for $D_p^U = 1.3 - 1.5$, $1.6 - 2.0$, $2.2 - 2.5$ m and $N_p^U = 30$

D_p^U	N_p^U	k	D_p	N_p	η_1	η_2	η_{ov_t}	v_{i_p}	Δp	c_{tot}
2.1	40	3	2.1	13	0.368	0.096	0.428	23.324	1321.739	0.019
2.2	40	3	2.2	12	0.368	0.096	0.428	24.434	1450.616	0.019
2.4	40	3	2.4	9	0.368	0.096	0.428	26.656	1726.353	0.018
2.5	40	3	2.5	10	0.314	0.079	0.368	21.953	1170.923	0.017

Table 4.14: Optimization result for $D_p^U = 2.1 - 2.2$, $2.4 - 2.5$ m and $N_p^U = 40$

The effects of varying the upper bound value of decision variables D_p^U and N_p^U in order to find the optimal value of the cyclone diameter and number of parallel lines can be seen in Figures 4.5 - 4.6. From these figures, while the optimal value of cyclone diameter lies at its upper bound, the optimal solution for the number of parallel lines lies within a wide range of values. These optimal values of D_p and N_p will be used by the GAMS algorithm to compute the optimal value of the pressure drop, inlet velocity, and total cost. It should be noted that a certain value of the upper bound of N_p can not be used in obtaining the feasible solutions for all relaxed NLP subproblems. For example, the optimal solution is only obtained by GAMS/DICOPT when using $N_p^U = 500$ along with the value of 0.3 m as the upper bound of cyclone diameter (D_p^U) (Table 4.5). As a result, the arrangement of 1D3D - 2D2D in series (level 3) is found as the best arrangement with $N_p = 489$ and $\eta_{ov_t} = 86.8$ % which is the maximum efficiency that can be attained for this optimization. The maximum value of the overall efficiency is actually constrained by the upper bound of 30 m/s being achieved by the inlet velocity. The resultant value of the total cost for this case is high (\$ 0.057 /second) because of the large number of the cyclones (i.e., 489 parallel lines x 2 series cyclone = 978 cyclones) with $D_p = 0.3$ m.
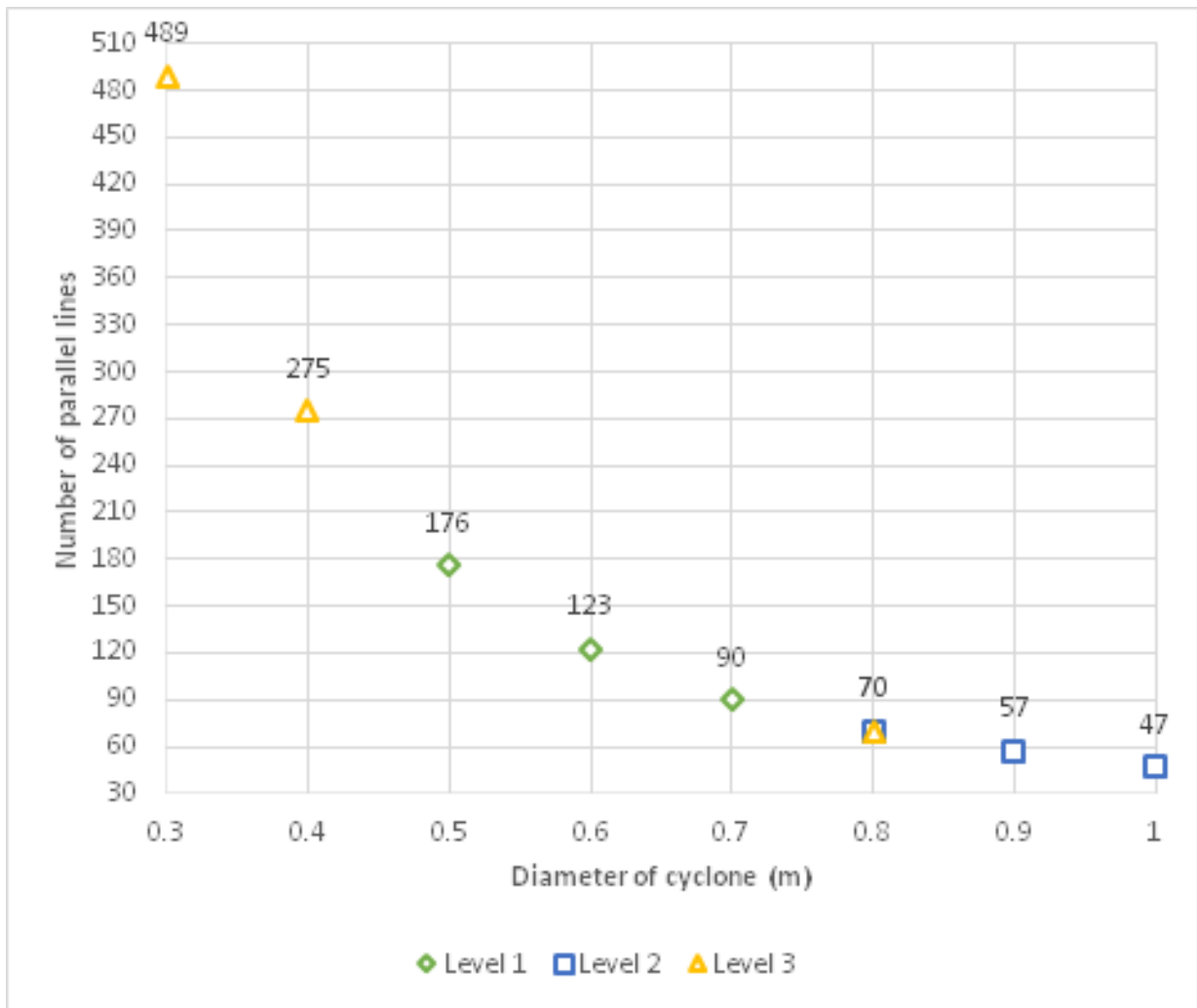
Figure 4.5: Optimal value of number of parallel lines vs diameter of the cyclone (1)
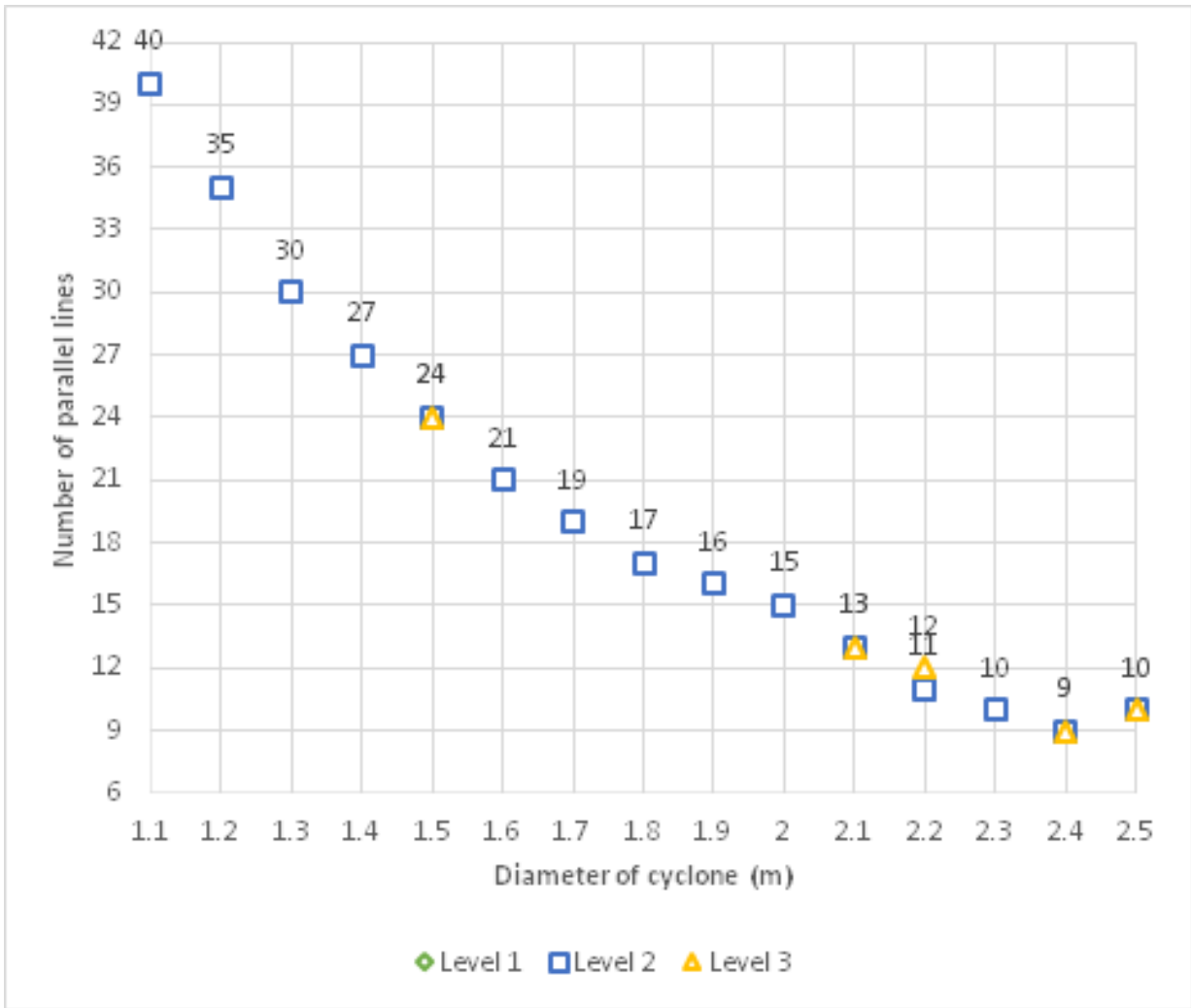
Figure 4.6: Optimal value of number of parallel lines vs diameter of the cyclone (2)

The maximum value of the overall efficiency of the cyclone arrangement that can be attained for a certain upper bound of the cyclone diameter is shown in Figure 4.7. The overall efficiency decreased nonlinearly as cyclone diameter increased with different slope of each level (cyclone arrangement) being chosen. The relationship between the overall efficiency and cyclone diameter in this optimization confirms the same relationship obtained by Faulkner et al. [27], who studied the effects of cyclone diameter on the collection efficiency of 1D3D cyclones. Moreover, a higher collection efficiency is accompanied by an increase in value of the inlet velocity and pressure drop across the cyclone, resulting in a higher total cost. Similar result were also reported by Gimbun et al. [41].

Figure 4.8 presents the relationship between the optimal value of the cyclone diameter and the minimum total cost achieved from the optimization. From this figure, an increase in the optimal value of D_p will result in a decrease in the total cost c_{tot}. This is because the operating cost is proportional to $\frac{1}{D^2}$ and even though the capital cost is proportional to diameter of the cyclone, a decreased value of the operating cost tends to be more dominant than the capital cost in obtaining the optimum total cost.
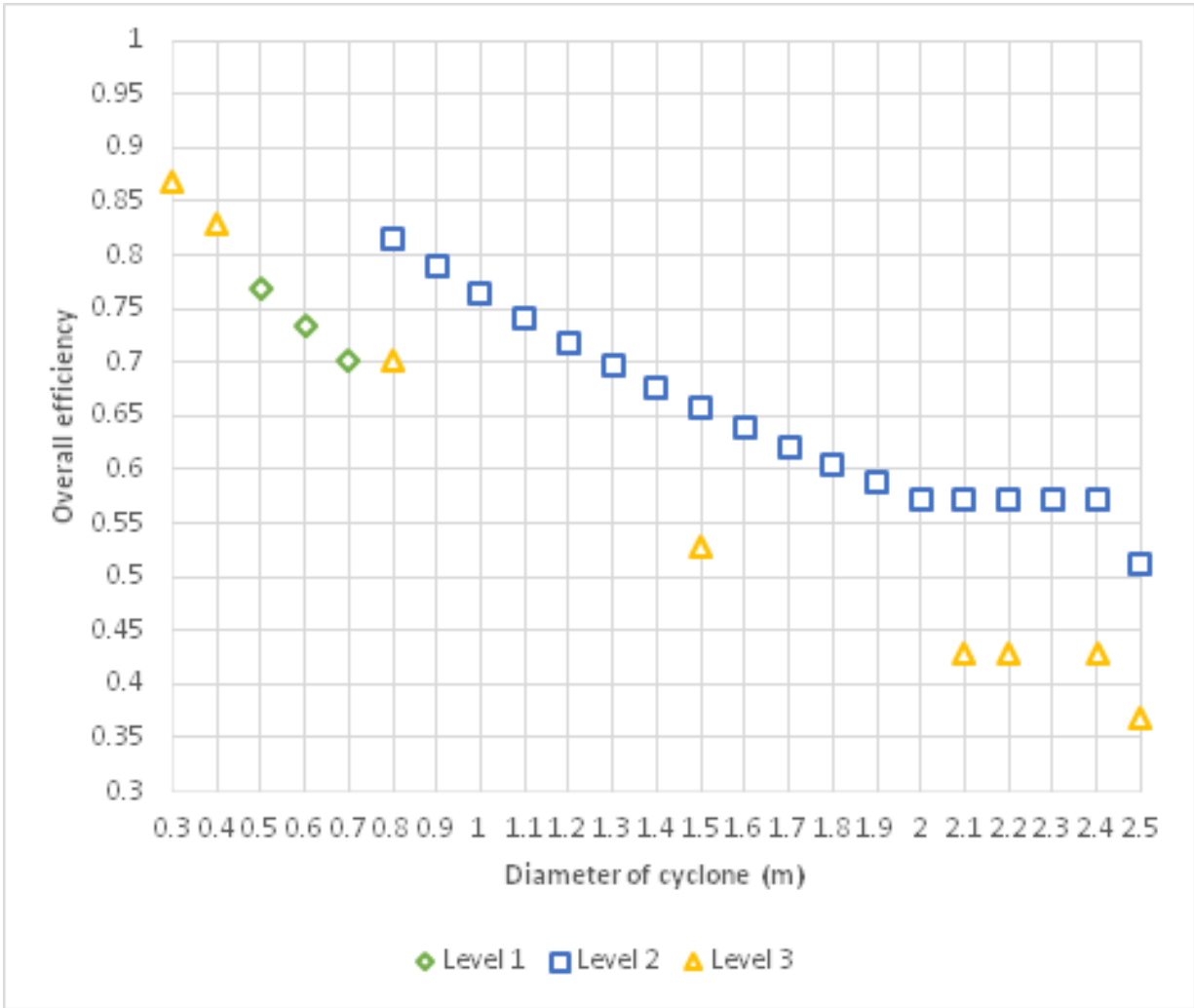
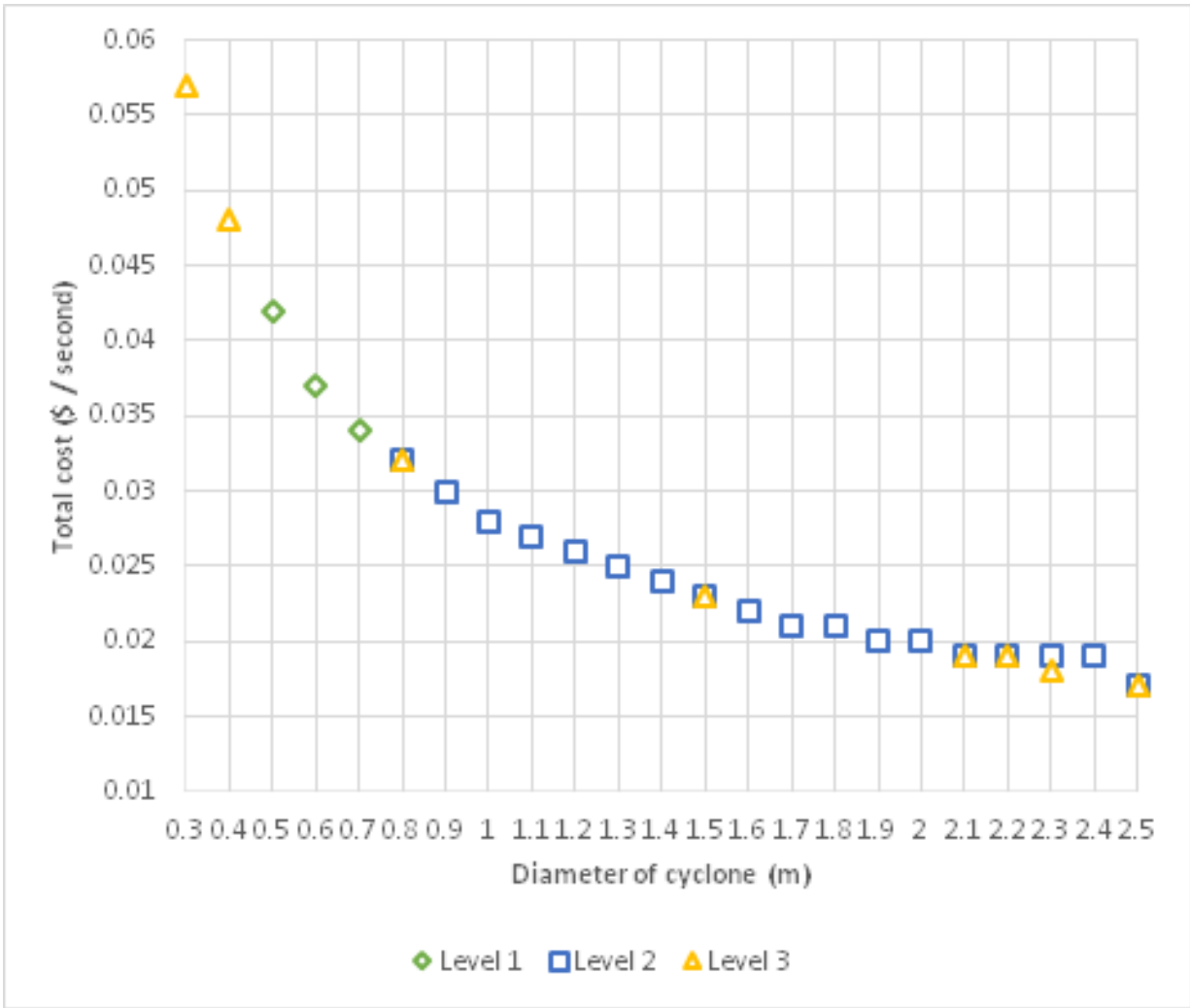Figure 4.7: Optimal value of the overall efficiency vs diameter of the cyclone

Figure 4.8: Total cost vs diameter of the cyclone

In addition, since the dimensions of the second cyclone would be the same as the first cyclone, the optimum efficiency of the second cyclones would have a lower value than the first cyclone. A lower value of the efficiency of the second cyclone compared to the first cyclone can be explained theoretically wherein by keeping the dimensions of the second cyclone to be similar to the first cyclone and as it is known that the calculation of the diameter of the second cyclone will be affected by the overall efficiency of the first cyclone (Eqs.(4.28-4.29)), the value of cut-size diameter of the second cyclone will increase to retain the value of the cyclone diameter. Thus, as can be seen in Figure 4.4, a higher value of the cut-size diameter will result in a lower value of the cyclone efficiency. So, the overall efficiency of the second cyclone shall not be higher than the value of the overall efficiency of the first cyclone. These results are found to be in line with the results reported by Whitelock and Buser [118], who studied the performance of multiple (up to four) 1D3D cyclones arranged in series.

It is interesting to observe from Figure 4.7 that there are only three from four levels available that have been chosen by the model as the best arrangement for a certain value of the decision variables D_p and N_p. For instance, with the resultant value of the efficiency more than 75 %, level 3 (1D3D+2D2D) is selected as the best cyclone arrangement for $D_p = 0.3$ - 0.4 m, level 1 (1D3D+1D3D) for $D_p = 0.5$ m, and level 2 (2D2D+2D2D) for $D_p = 0.8$ - 1.0 m. From the whole range, level 1 is available only when the value of D_p is in the range between 0.5 - 0.7 m. Meanwhile, level 2 is found being more dominant than the others in which it is selected as the best arrangement for a wide range value of the optimum diameter of the cyclone ($D_p = 0.8$ m to 2.5 m).

At a certain point, there are two levels selected as the best arrangement with the same D_p and N_p. For example, the upper bound value of 0.8 m, 1.5 m, 2.1 m, 2.4 m, and 2.5 m would result in two levels selected (i.e., level 2 and level 3) as the best arrangement with the same optimum number of parallel lines at each D_p. Another result shows that, the same two levels are selected as the best arrangement with the same $D_p = 2.2$ m, but with different value of N_p. The total costs associated with each levels (Figure 4.8) is found to be having the same value. Based on these results, two different types of cyclone arrangement

79

can be selected at the same cost but with different efficiencies (Figure 4.7) where the overall efficiency of cyclone arrangement on level 2 (2D2D+2D2D) is found higher than level 3 (1D3D+2D2D).

To further check the sensitivity of the decision variables to the optimal solutions, an additional optimization was also performed by using all the three decision variables (N, D_p, and η_{ov}). This optimization is also intended to computationally investigate the effect of η_{ov} if the bound is changed. In this case, the lower bound of the overall cyclone efficiency (η_{ov}^L) is set to have the initial value of 80 % and then increase in increments of 5 %. Meanwhile, a priori bounds of N_p^U and D_p^U are also selected. The optimal value of cyclone diameter and number of parallel lines for a given constraint of decision variable η_{ov} should lie within the bounds. Otherwise, a higher value of the upper bound (D_p^U and N_p^U) should be applied.

The computational results of the optimization are shown in Table 4.15. The method selects the lower bound of η_{ov} as the optimal value. The sensitivity of η_{ov} to the optimal solutions obtained from this optimization are found to be in accordance with the numerical findings from the previous study (Tables 4.5 - 4.14). For instance, as the cyclone diameter decreased along with the optimal value of inlet cyclone remains constant at its upper bound, the overall efficiency will increase. The optimal value of $\eta_{ov} = 90$ % obtained in this optimization is higher than the value of the previous optimization ($\eta_{ov} = 86.8$ %). It indicates that a higher η_{ov} is attainable by changing its lower bound until the optimal solution could be reached.

From Table 4.15, the model shows its consistency in selecting the cyclone arrangement of 1D3D+2D2D (level 3) as the best arrangement to obtain the optimal value of overall efficiency in the range of 80 % - 90 %. If these results are combined with the results given in Tables 4.5 - 4.6 (for $\eta_{ov} > 80$ %), it will complete the search for the optimal solution of level 3 to attain the maximum value of overall efficiency as presented in Table 4.16. However, the optimal solution for $\eta_{ov} = 90$ % (Table 4.15) provides two levels as the best arrangement, i.e., level 2 and 3. The cyclone arrangement of 2D2D+2D2D (level 2) will have a lower optimum number of parallel lines even though its dimensions are bigger than

the cyclone arrangement of 1D3D+2D2D (level 3). Consequently, the total cost of the cyclone arrangement of 2D2D+2D2D is lower than the 1D3D+2D2D, or in other words, the cyclone arrangement of 2D2D+2D2D is more efficient in total cost.

D_p^U	N_p^U	η_{ov}^L	η_{ov}^U	k	D_p	N_p	η_1	η_2	η_{ov_t}	v_{i_p}	Δp	c_{tot}
1	450	0.8	1	3	0.476	194	0.752	0.193	0.8	30	2186.78	0.043
1	450	0.85	1	3	0.344	373	0.813	0.2	0.85	30	2186.78	0.052
2	1000	0.9	1	3	0.226	861	0.875	0.202	0.9	30	2186.78	0.069
1	550	0.9	1	2	0.425	244	0.888	0.11	0.9	30	2186.78	0.046

Table 4.15: Optimization result using the decision variables N and η_{ov}

k	D_p	N_p	η_1	η_2	η_{ov_t}	v_{i_p}	Δp	c_{tot}
3	0.476	194	0.752	0.193	0.8	30	2186.78	0.043
3	0.4	275	0.786	0.197	0.828	30	2186.718	0.048
3	0.344	373	0.813	0.2	0.85	30	2186.78	0.052
3	0.3	489	0.835	0.201	0.868	30	2186.718	0.057
3	0.226	861	0.875	0.202	0.9	30	2186.78	0.069

Table 4.16: Complete results for level 3 as the best arrangement and η_{ov_t} = 80 % - 90 %

The optimization results obtained from the present mathematical programming models were also compared with the results from Ravi et al. [83], who studied a multi-objective optimization of a set of N identical reverse-flow cyclone separators in parallel by using the non-dominated sorting genetic algorithm (NSGA). Since they used nine decision variables in the optimization, compared to three decision variables in the present study, not all results would be presented. In particular, only the optimum solution of the number of parallel cyclones, cyclone diameter, and the efficiency of the cyclone are used for comparison. Table

4.17 lists comparisons of the optimal solution of decision variables, i.e., number of cyclone, diameter of the cyclone, and efficiency of the cyclone, where the results were evaluated using the same input feed (Table 4.3) and the same range of dimensions ratio of the cyclones (i.e., a_0, b_0, and D_{e_0}). It should be noted that there is no table provided in Ravi et al. [83] results, all the results presented in scatter charts instead. Hence, the values listed in Table 4.17 are rough estimated number from those charts provided.

η	Present study		Ravi et al.	
	Number of cyclone	D (m)	Number of cyclone	D (m)
77%	352	0.5	1400	0.3
80%	388	0.476	1600	0.3
85%	746	0.344	1300	0.3

Table 4.17: Comparison of the optimal solution of decision variables

The comparisons illustrated that the present study gave the lower number of parallel cyclones for the same value of the efficiency of the cyclone. In addition, the optimum efficiency of the cyclone that can be achieved from the present study (90 %) is slightly higher than Ravi et al. [83]. Based on the above comparisons, it can be concluded that the optimization of the cyclone arrangement in parallel-series using 1D3D and/or 2D2D cyclones found to be a novel solution among other pollution control strategies to reduce the pollution to the minimum level.

4.5   Chapter Summary

This chapter presented a MINLP (Mixed Integer Nonlinear Programming) model to find the best cyclone arrangement with the optimal number and configuration / dimensions

of the cyclone from four combinations of 1D3D and 2D2D cyclones arranged in parallel-series. The cyclone arrangement is optimized with respect to the minimum total cost which includes the operating cost and capital cost. The proposed model is implemented to handle a total flow rate of 165 m^3/s of a stream to be processed in a paper mill. The MINLP problem was carried out using DICOPT that runs under GAMS, while the MILP master problem and NLP subproblem were solved using CPLEX and CONOPT 3, respectively. Three decision variables (N, D, and η_{ov}) were involved in selecting the best cyclone arrangement from four levels available (1D3D+1D3D, 2D2D+2D2D, 1D3D+2D2D, and 2D2D+1D3D). It was found that D is the important decision variable that led the model to obtain the optimal solution. Different values used for the upper bound of D and N results in three different cyclone arrangements selected as the optimal solution. The sensitivity of the decision variables to the optimal solution is described as follows: the overall efficiency of the cyclone as well as the optimal number of the cyclone will decrease as the cyclone diameter increases, followed by a decrease in the total cost. As a result of this study, the parallel-series cyclone arrangement of 2D2D+2D2D is found to be more economical and efficient compared to the others.

Chapter 5

Conclusions and Recommendations

The use of multiple cyclones can be considered as one solution to the demands of obtaining the best pollution control strategies to achieve a minimum level of pollution reduction. In order to give the best solution in designing an optimum arrangement and dimensions of the cyclone, there is a need to develop an effective mathematical programming combined with the use of modern tools of optimization. A summary of the findings of new methods to the solution of cyclone arrangement problems is presented in Section 5.1. Recommendations for future work in this field are discussed in Section 5.2.

5.1   Conclusion

Mathematical programming models aimed at obtaining the best configuration of multiple cyclone arrangement has been developed. The key idea of the present mathematical programming model is to present the capability of General Algebraic Modeling System (GAMS) software in solving multiple cyclone arrangement problems. Two mathematical programming techniques are used to optimize different cyclone arrangement i.e., nonlinear programming (NLP) model for 1D3D, 2D2D, and 1D2D cyclones in parallel or in series and mixed integer nonlinear programming (MINLP) model for four combinations of 1D3D

and 2D2D cyclones arranged in parallel-series. The objective of all these models is to find the optimal number and dimensions of cyclone arrangement with respect to the minimum total cost including the operating cost and the capital cost.

The proposed model of nonlinear programming optimization of series and parallel cyclone arrangement is applied in NPK (Nitrogen, Phosphorus, and Potassium) fertilizer plant. Different types of cyclones, in parallel or in series arrangements, result in different optimal numbers of cyclones. Each type of cyclone (i.e., 1D3D, 2D2D, and 1D2D) has an alternative that can be arranged either in parallel or in series configuration. The cyclone diameter becomes a basic consideration because it determines the overall size of the cyclone, especially for the cyclone height. Therefore, if the available space is limited on the field, it is advised to choose the small cyclone with a small number of the cyclone arrangement. The 1D3D cyclones connected in parallel have the smallest diameter for the same value of optimal number of cyclones (N = 3) compared with the other two. The 1D2D cyclone in a series is more suitable to handle a given input feed of which it has the lowest pressure drop with the smallest size of diameter (i.e., 2.5 m) compared to the others. In addition, two cyclones in series is more likely to be operated than three cyclones because the total cost of three cyclones in series is higher than the two cyclones.

A MINLP (Mixed Integer Nonlinear Programming) model to find the best cyclone arrangement with the optimal number of cyclones and dimensions from four combinations of 1D3D and 2D2D cyclones arranged in parallel-series has been successfully developed. Three decision variables (N, D, and η_{ov}) have a strong influence in selecting the best cyclone arrangement from four levels available (1D3D+1D3D, 2D2D+2D2D, 1D3D+2D2D, and 2D2D+1D3D). Different values used for the upper bound of D and N would result in different cyclone arrangement selected as the optimal solution. The sensitivity results of the decision variables to the optimal solution are found in line with the results obtained from other researcher who studied in the same area by experimentally or computationally. The optimum value of 90 % of the overall efficiency for a given feed with a high volume and heavy loading of solid particles ($Q = 165 \ m/s$ and $\rho_p = 1600 \ kg/m^3$) can be attained either by 1D3D+2D2D cyclones arrangement or 2D2D+2D2D cyclones arrangement in parallel-

series with different dimensions and number of the cyclone. The cyclone arrangement of 2D2D+2D2D in parallel-series is found to be the best arrangement with a higher efficiency and a lower total cost compared to the others.

5.2 Recommendations

The research presented in this work can be extended further to increase its contribution to the field of optimal multiple cyclone arrangement. Some of the recommendations for the way forward of this research are discussed below.

- General Algebraic Modeling System (GAMS) software in solving multiple cyclone arrangement problems in this work has proved its capability to handle a nonlinearity in multiple cyclone arrangement problem then produce an optimal solution of the optimal number, dimensions, and the best cyclone arrangement. Although this work has produce an optimal solution for cyclone arrangement problem, there are several assumptions involved in the optimization. For example, since all the equations used in this work derived from the time-of-flight model and no cut-size diameter correction factor was found in the literature for its model, the correction factor for equilibrium-orbit model (the model of Barth) was used in the cut-size diameter equation. Therefore, an experiment in order to find a correction factor to modify the theoretical cut-size diameter of time-of-flight model to quantify the effect of PSD on the cut-size diameter calculation is recommended for future work.

- It is known that the efficiency of cyclone systems is a function of the particle size distribution (PSD) of entrained dust to the cyclone. In this work, due to limitations of available data in the literature, the PSD of the particles of the feed entered to the second cyclone in series of all type of cyclones was assumed to be the same with the experimental result of 1D3D+1D3D cyclones. Additional optimization using different PSD data that enter to the second cyclone for other combinations of cyclones (i.e.,

1D3D+2D2D, 2D2D+2D2D, 2D2D+1D3D) and actual field tests are recommended as part of the future work in this research.

- The study presented in this work made use of three types of cyclone, i.e., 1D3D, 2D2D, and 1D2D cyclone. Expanding the study to address the optimal solution of multiple cyclone arrangement in parallel, series, and parallel-series using combinations of a wide range type of the cyclone is recommended for future work.

- The optimization results using GAMS software which have been obtained in the present work, allowing for more effective and optimal solution of a greater complexity of the cyclone arrangement problem in the future.

APPENDICES

A   Copyright Release

The contents of Chapter 3 has been published in the Powder Technology [2]. The author of this thesis is the main author of this publication and contributed all the technical aspects of the work as well as writing the manuscript. Permission to reuse the content of the article has been granted by the publisher (see Figure A.1).

B   MATLAB code

```
M = [10e-6]*1e6;
G = [2.5];
for k = 1:1
xlimit = [1e-6 14e-6]*1e6;
step = 1e-7*1e6;
fun = @(x) 1./(sqrt(2.*pi).*x.*log(G(k))).*exp(-0.5.*((log(x)-log(M(k)))./
log(G(k))).^2);
fun2 = @(x) integral(fun,x,inf);
figure(1)
ezplot(fun2,xlimit)
xlabel('Cut-size Diameter')
```

```
ylabel('Efficiency')
grid on

hold all
j = 0;

end
----------------------------------------
M = [3.7e-6]*1e6;
G = [2.5];
for k = 1:1
xlimit = [1e-7 10e-6]*1e6;
step = 1e-7*1e6;
fun = @(x) 1./(sqrt(2.*pi).*x.*log(G(k))).*exp(-0.5.*((log(x)-log(M(k)))./
log(G(k))).^2);
fun2 = @(x) integral(fun,x,inf);
figure(1)
ezplot(fun2,xlimit)
xlabel('Cut-size Diameter')
ylabel('Efficiency')
grid on

hold all
j = 0;

end
```

Figure A.1: License agreement copy from Elsevier to reuse content of article

90

References

[1] GAMS-CPLEX solver description.

[2] Sabah Ahmed Abdul-Wahab, Muhamad Fariz Failaka, Lena Ahmadi, Ali Elkamel, and Kaan Yetilmezsoy. Nonlinear programming optimization of series and parallel cyclone arrangement of npk fertilizer plants. *Powder Technology*, 264:203–215, 2014.

[3] R McK Alexander. Fundamentals of cyclone design and operation. *Proc. Aus. Inst. Min. Met. NS*, 152(3):152–153, 1949.

[4] Ioannis P Androulakis, Costas D Maranas, and Christodoulos A Floudas. αbb: A global optimization method for general constrained nonconvex problems. *Journal of Global Optimization*, 7(4):337–363, 1995.

[5] A Avci and I Karagoz. Theoretical investigation of pressure losses in cyclone separators. *International communications in heat and mass transfer*, 28(1):107–117, 2001.

[6] W Barth. Design and layout of the cyclone separator on the basis of new investigations. *Brenn. Warme Kraft*, 8:1–9, 1956.

[7] Jaime Benítez. *Process engineering and design for air pollution control*. Prentice Hall, 1993.

[8] V Bhaskar, Santosh K Gupta, and Ajay K Ray. Applications of multiobjective optimization in chemical engineering. *Reviews in Chemical Engineering*, 16(1):1–54, 2000.

[9] R Byron Bird, Warren E Stewart, and Edwin N Lightfoot. *Transport phenomena*. John Wiley & Sons, 2007.

[10] Anthony J Buonicore and Wayne T Davis. *Air pollution engineering manual*. Van Nostrand Reinhold, 1992.

[11] Joaquin Casal and Jose M Martinez-Benet. Better way to calculate cyclone pressure drop. *Chemical engineering*, 90(2):99–100, 1983.

[12] Jianyi Chen and Mingxian Shi. A universal model to calculate cyclone pressure drop. *Powder technology*, 171(3):184–191, 2007.

[13] Amy R Ciric and Deyao Gu. Synthesis of nonequilibrium reactive distillation processes by minlp optimization. *AIChE Journal*, 40(9):1479–1487, 1994.

[14] Roland Clift, John R Grace, and Martin E Weber. *Bubbles, drops, and particles*. Courier Corporation, 2005.

[15] EP Columbus. Series cyclone arrangements to reduce gin emissions. *Transactions of the ASAE (USA)*, 1993.

[16] JJ Derksen. Separation performance predictions of a stairmand high-efficiency cyclone. *AIChE Journal*, 49(6):1359–1371, 2003.

[17] John Dirgo and David Leith. Cyclone collection efficiency: comparison of experimental results with theoretical predictions. *Aerosol Science and Technology*, 4(4):401–415, 1985.

[18] LCW Dixon. *Global optima without convexity*. Numerical Optimisation Centre, Hatfield Polytechnic, 1977.

[19] LCW Dixon and GP Szegö. The global optimization problem: an introduction. *Towards global optimization*, 2:1–15, 1978.

[20] Arne Drud. GAMS-CONOPT solver description.

[21] MA Duran and IE Grossmann. A mixed-integer nonlinear programming algorithm for process systems synthesis. *AIChE journal*, 32(4):592–606, 1986.

[22] Marco A Duran and Ignacio E Grossmann. An outer-approximation algorithm for a class of mixed-integer nonlinear programs. *Mathematical programming*, 36(3):307–339, 1986.

[23] Alexia A Economopoulou and Alexander P Economopoulos. Method for estimating size-specific particulate emission inventories. *Journal of environmental engineering*, 127(12):1139–1148, 2001.

[24] Thomas GW Epperly and Ross E Swaney. Branch and bound for global nlp: New bounding lp. *Nonconvex Optimization and Its Applications*, 9:1–36, 1996.

[25] Grossmann et al. GAMS-DICOPT solver description.

[26] WB Faulkner and BW Shaw. Efficiency and pressure drop of cyclones across a range of inlet velocities. *Applied engineering in agriculture*, 22(1):155, 2006.

[27] William B Faulkner, Michael D Buser, Derek P Whitelock, and Bryan W Shaw. Effects of cyclone diameter on performance of 1d3d cyclones: collection efficiency. *Transactions of the ASABE*, 50(3):1053–1059, 2007.

[28] MW First. Cyclone dust collector design. In *Am. Soc. Mech. Eng*, volume 49, pages 127–132, 1949.

[29] Roger Fletcher and Sven Leyffer. Solving mixed integer nonlinear programs by outer approximation. *Mathematical programming*, 66(1-3):327–349, 1994.

[30] CA Floudas, A Aggarwal, and AR Ciric. Global optimum search for nonconvex nlp and minlp problems. *Computers & Chemical Engineering*, 13(10):1117–1132, 1989.

[31] CA Floudas and AR Ciric. Strategies for overcoming uncertainties in heat exchanger network synthesis. *Computers & Chemical Engineering*, 13(10):1133–1152, 1989.

[32] CA Floudas and GE Paules. A mixed-integer nonlinear programming formulation for the synthesis of heat-integrated distillation sequences. *Computers & chemical engineering*, 12(6):531–546, 1988.

[33] CA Floudas and V Visweswaran. A global optimization algorithm (gop) for certain classes of nonconvex nlpsi. theory. *Computers & chemical engineering*, 14(12):1397–1417, 1990.

[34] Christodoulos A Floudas and Avanish Aggarwal. A decomposition strategy for global optimum search in the pooling problem. *ORSA Journal on Computing*, 2(3):225–235, 1990.

[35] Christodoulos A Floudas and Vishy Visweswaran. Primal-relaxed dual global optimization approach. *Journal of Optimization Theory and Applications*, 78(2):187–225, 1993.

[36] PA Funk, RW Clifford, and SE Hughs. Optimum entry velocity for modified 1d3d cyclones. In *ASAE Paper No. 994198*. 1999.

[37] Arthur M Geoffrion. Generalized benders decomposition. *Journal of optimization theory and applications*, 10(4):237–260, 1972.

[38] AM Gerrard and CJ Liddle. The optimal choice of multiple cyclones. *Powder Technology*, 13(2):251–254, 1976.

[39] MN Gillum and SE Hughs. Velocity effects on operating parameters of series cyclones. *Transactions of the ASAE*, 26(2):606–609, 1983.

[40] MN Gillum, SE Hughs, and BM Armijo. Use of secondary cyclones for reducing gin emissions. *Transactions of the ASAE*, 25(1):210–213, 1982.

[41] Jolius Gimbun, TG Chuah, Thomas SY Choong, and A Fakhru'l-Razi. A cfd study on the prediction of cyclone collection efficiency. *International Journal for Computational Methods in Engineering Science and Mechanics*, 6(3):161–168, 2005.

[42] Jolius Gimbun, TG Chuah, A Fakhrul-Razi, and Thomas SY Choong. The influence of temperature and inlet velocity on cyclone pressure drop: a cfd study. *Chemical Engineering and Processing: Process Intensification*, 44(1):7–12, 2005.

[43] WD Griffiths and F Boysan. Computational fluid dynamics (cfd) and empirical modelling of the performance of a number of cyclone samplers. *Journal of Aerosol Science*, 27(2):281–304, 1996.

[44] Ignacio E Grossmann. Mixed-integer programming approach for the synthesis of integrated process flowsheets. *Computers & chemical engineering*, 9(5):463–482, 1985.

[45] Ignacio E Grossmann. Mixed-integer nonlinear programming techniques for the synthesis of engineering systems. *Research in Engineering Design*, 1(3-4):205–228, 1990.

[46] Ignacio E Grossmann. Mixed-integer optimization techniques for algorithmic process synthesis. *Advances in Chemical Engineering*, 23:171–246, 1996.

[47] Ignacio E Grossmann. Review of nonlinear mixed-integer and disjunctive programming techniques. *Optimization and Engineering*, 3(3):227–252, 2002.

[48] Ignacio E Grossmann et al. Minlp optimization strategies and algorithms for process synthesis. 1989.

[49] Ignacio E Grossmann and Zdravko Kravanja. Mixed-integer nonlinear programming techniques for process systems engineering. *Computers & Chemical Engineering*, 19:189–204, 1995.

[50] Ignacio E Grossmann and Jorge Santibanez. Applications of mixed-integer linear programming in process synthesis. *Computers & Chemical Engineering*, 4(4):205–214, 1980.

[51] Omprakash K Gupta and A Ravindran. Branch and bound experiments in convex nonlinear integer programming. *Management science*, 31(12):1533–1546, 1985.

[52] AJ Hoekstra, JJ Derksen, and HEA Van Den Akker. An experimental and numerical study of turbulent swirling flow in gas cyclones. *Chemical Engineering Science*, 54(13):2055–2065, 1999.

[53] Arjen Jacco Hoekstra. *Gas flow field and collection efficiency of cyclone separators.* PhD thesis, TU Delft, Delft University of Technology, 2000.

[54] AC Hoffmann, M De Groot, W Peng, HWA Dries, and J Kater. Advantages and risks in increasing cyclone separator length. *AIChE journal*, 47(11):2452–2460, 2001.

[55] AC Hoffmann and LE Stein. Gas cyclones and swirl tubes: Principles. *Design and Operation, 2nd Edition Springer*, 2008.

[56] Reiner Horst and Hoang Tuy. *Global optimization: Deterministic approaches.* Springer Science & Business Media, 2013.

[57] Donna Lee Iozia and David Leith. Effect of cyclone dimensions on gas flow pattern and collection efficiency. *Aerosol Science and Technology*, 10(3):491–500, 1989.

[58] B Kalen and FA Zenz. Theoretical-empirical approach to saltation velocity in cyclone design. In *AIChE Symposium Series*, volume 70, pages 388–396, 1974.

[59] Irfan Karagoz and Atakan Avci. Modelling of the pressure drop in tangential inlet cyclone separators. *Aerosol Science and Technology*, 39(9):857–865, 2005.

[60] LC Kenny and RA Gussman. A direct approach to the design of cyclones for aerosol-monitoring applications. *Journal of aerosol science*, 31(12):1407–1420, 2000.

[61] Wolfgang H KOCH and William LICHT. New design approach boosts cyclone efficiency. *Chemical engineering*, 84(24):80–88, 1977.

[62] Gary R Kocis and Ignacio E Grossmann. Relaxation strategy for the structural optimization of process flow sheets. *Industrial & engineering chemistry research*, 26(9):1869–1880, 1987.

[63] Gary R Kocis and Ignacio E Grossmann. Global optimization of nonconvex mixed-integer nonlinear programming (minlp) problems in process synthesis. *Industrial & Engineering Chemistry Research*, 27(8):1407–1421, 1988.

[64] E Kondili, CC Pantelides, and RWH Sargent. A general algorithm for short-term scheduling of batch operationsi. milp formulation. *Computers & Chemical Engineering*, 17(2):211–227, 1993.

[65] Zdravko Kravanja and Ignacio E Grossmann. Prosynan minlp process synthesizer. *Computers & chemical engineering*, 14(12):1363–1378, 1990.

[66] Hong Ming Ku and Iftekhar A Karimi. Scheduling in serial multiproduct batch processes with finite interstage storage: mixed integer linear program formulation. *Industrial & engineering chemistry research*, 27(10):1840–1848, 1988.

[67] Ashwani Kumar and Angelo Lucia. Separation process optimization calculations. *Applied numerical mathematics*, 3(5):409–425, 1987.

[68] David Leith and William Licht. The collection efficiency of cyclone type particle collectors: a new theoretical approach. In *AIChE Symp. Ser*, volume 68, pages 196–206, 1972.

[69] KS Lim, HS Kim, and KW Lee. Characteristics of the collection efficiency for a cyclone with different vortex finder shapes. *Journal of Aerosol science*, 35(6):743–754, 2004.

[70] A Lucia, J Xu, and KM Layn. Nonconvex process optimization. *Computers & chemical engineering*, 20(12):1375–1398, 1996.

[71] VASILIOS MANOUSIOUTHAKIS and DENNIS SOURLAS. A global optimization approach to rationally constrained rational programming. *Chemical Engineering Communications*, 115(1):127–147, 1992.

[72] JM Martinez-Benet and J Casal. Optimization of parallel cyclones. *Powder technology*, 38(3):217–221, 1984.

[73] A Mauderli and DWT Rippin. Production planning and scheduling for multi-purpose batch chemical plants. *Computers & Chemical Engineering*, 3(1):199–206, 1979.

[74] Soterios A Papoulias and Ignacio E Grossmann. A structural optimization approach in process synthesisiii: total processing systems. *Computers & chemical engineering*, 7(6):723–734, 1983.

[75] CB Parnell Jr and DD Davis. Predicted effects of the use of new cyclone designs on agricultural processing particulate emissions. In *ASAE Southwest Region Meeting. St. Joseph, Mich.: ASAE*, 1979.

[76] W Peng, AC Hoffmann, PJAJ Boot, A Udding, HWA Dries, A Ekker, and J Kater. Flow pattern in reverse-flow centrifugal separators. *Powder Technology*, 127(3):212–222, 2002.

[77] F Pettersson and T Westerlund. Global optimization of pump configurations using binary separable programming. *Computers & chemical engineering*, 21(5):521–529, 1997.

[78] JM Pinto and IE Grossmann. Optimal cyclic scheduling of multistage continuous multiproduct plants. *Computers & Chemical Engineering*, 18(9):797–816, 1994.

[79] Jose M Pinto and Ignacio E Grossmann. A continuous time mixed integer linear programming model for short term scheduling of multistage batch plants. *Industrial & Engineering Chemistry Research*, 34(9):3037–3051, 1995.

[80] Ignacio Quesada and Ignacio E Grossmann. An lp/nlp based branch and bound algorithm for convex minlp optimization problems. *Computers & chemical engineering*, 16(10):937–947, 1992.

[81] Ignacio Quesada and Ignacio E Grossmann. A global optimization algorithm for linear fractional and bilinear programs. *Journal of Global Optimization*, 6(1):39–76, 1995.

[82] G Ramachandran, David Leith, John Dirgo, and Henry Feldman. Cyclone optimization based on a new empirical model for pressure drop. *Aerosol Science and Technology*, 15(2):135–148, 1991.

[83] G Ravi, Santosh K Gupta, and MB Ray. Multiobjective optimization of cyclone separators using genetic algorithm. *Industrial & engineering chemistry research*, 39(11):4272–4286, 2000.

[84] Steven H Rich and George J Prokopakis. Scheduling and sequencing of batch operations in a multipurpose plant. *Industrial & Engineering Chemistry Process Design and Development*, 25(4):979–988, 1986.

[85] K Rietema. Het mechanisme van de afscheiding van fijnverdeelde stoffen in cyclonen. *De Ingenieur*, 71:39, 1959.

[86] Richard E Rosenthal. Gams–a user's guide. 2004.

[87] P Rosin, E Rammler, and W Intelmann. Principles and limits of cyclone dust removal. *Zeit. Ver. Deutscher Ing*, 76:433–437, 1932.

[88] Hong S Ryoo and Nikolaos V Sahinidis. Global optimization of nonconvex nlps and minlps with applications in process design. *Computers & Chemical Engineering*, 19(5):551–566, 1995.

[89] Hong S Ryoo and Nikolaos V Sahinidis. A branch-and-reduce approach to global optimization. *Journal of Global Optimization*, 8(2):107–138, 1996.

[90] NV Sahinidis and Ignacio E Grossmann. Minlp model for cyclic multiproduct scheduling on continuous parallel lines. *Computers & chemical engineering*, 15(2):85–103, 1991.

[91] RWH Sargent and K Gaminibandara. Optimum design of plate distillation columns. *Optimization in action*, pages 267–314, 1976.

[92] HI Shaban, A Elkamel, and R Gharbi. An optimization model for air pollution control decision making. *Environmental Modelling & Software*, 12(1):51–58, 1997.

[93] N Shah, CC Pantelides, and RWH Sargent. A general algorithm for short-term scheduling of batch operationsii. computational issues. *Computers & Chemical Engineering*, 17(2):229–244, 1993.

[94] CB Shepherd and CE Lapple. Air pollution control: a design approach. *Cyclones, second ed., Woveland Press Inc., Illinois*, pages 127–139, 1939.

[95] CB Shephered and CE Lapple. Flow pattern and pressure drop in cyclone dust collectors. *Industrial & Engineering Chemistry*, 31(8):972–984, 1939.

[96] S Simpson and CB Parnell Jr. New low-pressure cyclone design for cotton gins. In *Proc. 1995 Beltwide Cotton Production Conferences*, pages 680–687, 1995.

[97] R.K. Sinnott. *Chemical Engineering Design*. Elsevier Butterworth-Heinemann, 2005.

[98] Edward MB Smith and Constantinos C Pantelides. Global optimisation of general process models. In *Global optimization in engineering design*, pages 355–386. Springer, 1996.

[99] Robin M Smith. *Chemical process: design and integration.* John Wiley & Sons, 2005.

[100] Giulio Solero and Aldo Coghe. Experimental fluid dynamic characterization of a cyclone chamber. *Experimental thermal and fluid science*, 27(1):87–96, 2002.

[101] C J. Stairmand. The design and performance of cyclone separators. *Trans. Inst. Chem. Eng*, 29:356–383, 1951.

[102] George Stephanopoulos and Arthur W Westerberg. The use of hestenes' method of multipliers to resolve dual gaps in engineering system optimization. *Journal of Optimization Theory and Applications*, 15(3):285–309, 1975.

[103] Prabhata K Swamee, Nitin Aggarwal, and Kuldeep Bhobhiya. Optimum design of cyclone separator. *AIChE journal*, 55(9):2279–2283, 2009.

[104] RE Swaney. Global solution of algebraic nonlinear programs. In *AIChE Annual Meeting, Chicago, IL*, 1990.

[105] Gifford H Symonds. *Linear programming: the solution of refinery problems.* Esso Standard Oil Company, 1955.

[106] Athanasios G Tsirukis, Savoula Papageorgaki, and Gintaras V Reklaitis. Scheduling of multipurpose batch chemical plants with resource constraints. *Industrial & engineering chemistry research*, 32(12):3037–3050, 1993.

[107] R Vaidyanathan and M El-Halwagi. Global optimization of nonconvex nonlinear programs via interval analysis. *Computers & Chemical Engineering*, 18(10):889–897, 1994.

[108] Jagadisan Viswanathan and Ignacio E Grossmann. A combined penalty function and outer-approximation method for minlp optimization. *Computers & Chemical Engineering*, 14(7):769–782, 1990.

[109] Jagadisan Viswanathan and Ignacio E Grossmann. An alternate minlp model for finding the number of trays required for a specified separation objective. *Computers & chemical engineering*, 17(9):949–955, 1993.

[110] Jagadisan Viswanathan and Ignacio E Grossmann. Optimal feed locations and number of trays for distillation columns with multiple feeds. *Industrial & engineering chemistry research*, 32(11):2942–2949, 1993.

[111] L Wang, CB Parnell, BW Shaw, and RE Lacey. Analysis of cyclone collection efficiency. In *Proceedings of 2003 ASAE Annual International Meeting, Las Vegas, Paper*, volume 34114, 2003.

[112] L Wang, CB Parnell, BW Shaw, and RE Lacey. A theoretical approach for predicting number of turns and cyclone pressure drop. *Transactions of the ASABE*, 49(2):491–503, 2006.

[113] Lingjuan Wang, Calvin B Parnell, and Bryan W Shaw. Performance characteristics of cyclones in cotton-gin dust removal. *Agricultural Engineering International: CIGR EJournal.*, 2002.

[114] Lingjuan Wang, Calvin B Parnell, and Bryan W Shaw. Study of the cyclone fractional efficiency curves. *Agricultural Engineering International: CIGR EJournal.*, 2002.

[115] Lingjuan Wang, CB Parnell, and Bryan W Shaw. 1d2d, 1d3d, 2d2d cyclone fractional efficiency curves for fine dust. In *Proc. 2000 Beltwide Cotton Production Conferences*, 2000.

[116] Tapio Westerlund and Frank Pettersson. *A cutting plane method for solving convex MINLP problems*. Åbo Akademi, 1994.

[117] Tapio Westerlund, Frank Pettersson, and Ignacio E Grossmann. Optimization of pump configurations as a minlp problem. *Computers & chemical engineering*, 18(9):845–858, 1994.

[118] DP Whitelock and MD Buser. Multiple series cyclones for high particulate matter concentrations. *Applied engineering in agriculture*, 23(2):131, 2007.

[119] Rongbiao Xiang, SH Park, and KW Lee. Effects of cone dimension on cyclone performance. *Journal of Aerosol Science*, 32(4):549–561, 2001.

[120] Wen-ching Yang. *Handbook of fluidization and fluid-particle systems*. CRC press, 2003.

[121] Kaan Yetilmezsoy. Optimisation using prediction models: air cyclones' body diameter/pressure drop. *Filtration & Separation*, 42(10):32–35, 2005.

[122] Kaan Yetilmezsoy. Determination of optimum body diameter of air cyclones using a new empirical model and a neural network approach. *Environmental engineering science*, 23(4):680–690, 2006.

[123] BINGTAO Zhao. A theoretical approach to pressure drop across cyclone separators. *Chemical engineering & technology*, 27(10):1105–1108, 2004.